Spin State Modulation of Iron Spin Crossover Complexes Via Hydrogen-Bonding Self-Assembly

Michael C. Young, Erica Liew, Jonathan Ashby, Kelsi M. McCoy and Richard J. Hooley.*

Department of Chemistry, University of California, Riverside, CA 92521.

richard.hooley@ucr.edu

Supporting Information

1. General Information

^{1}H and ^{13}C spectra were recorded on a Varian Inova 400 MHz or Varian Inova 500 MHz NMR spectrometer. Proton (^{1}H) chemical shifts are reported in parts per million (δ) with respect to tetramethylsilane (TMS, δ=0), and referenced internally with respect to the protio solvent impurity. The ^{13}C NMR of paramagnetic complexes (specifically those of iron(II)) could not be acquired at room temperature due to broadening, and at lower temperatures the decreased solubility prevented spectral acquisition in a reasonable amount of time. Magnetic susceptibility measurements were performed according to the Evans method, with the deuterated solvent used as the reference, and the chemical shift difference between the reference and solution used to determine the paramagnetic contribution of the solute.[1] Deuterated NMR solvents were obtained from Cambridge Isotope Laboratories, Inc., Andover, MA, and used without further purification. Mass spectra were recorded on an Agilent 6210 LC TOF mass spectrometer using electrospray ionization with fragmentation voltage set at 115 V and processed with an Agilent MassHunter Operating System. Room temperature UV/Vis spectroscopy was performed on a Cary 50 Photospectrometer using the Varian Scans program to collect data. Variable temperature UV/Vis spectra were obtained by suspending a cuvette in a dewar filled with an acetone/dry ice bath for low temperatures and a heated beaker of water for warmer temperatures, with spectra collected using a home-built Ocean Optics system. All other materials were obtained from Aldrich Chemical Company, St. Louis, MO and were used as received. Cyclic voltammetry was performed using a CH Instruments Electrochemical Analyzer with a glassy carbon working electrode, a Pt wire auxiliary, and Ag/AgCl for the reference electrode. Solvents were dried through a commercial solvent purification system (Pure Process Technologies, Inc.). Molecular modeling (semi-empirical calculations) was performed using the AM1 force field using SPARTAN.[2]

2. Synthesis of Compounds

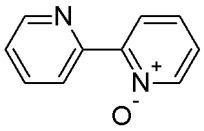

2,2'-Bipyridyl-N-Oxide (*S-1*):

2,2'-Bipyridine (1.248 g, 8.00 mmol) was added to a 50 mL round-bottomed flask with stir bar, followed by dissolution in trifluoroacetic acid (6.0 mL). This was cooled to room temperature, followed by slow addition of 30% H_2O_2 (1.2 mL, 12 mmol). Reaction was stirred at room temperature for 2 h, followed by addition of chloroform (25 mL). This was washed with 6M aqueous NaOH (3 x 10 mL), followed by back extraction of the combined aqueous phase with dichloromethane (4 x 20 mL). The combined organic phase was dried over $MgSO_4$, followed by evaporation *in vacuo* to give an oil. This was dried under vacuum overnight to give a beige solid (1.25 g, 91%). ^{1}H NMR (400 MHz; $CDCl_3$) δ 8.90 (d, J = 8.0 Hz, 1H), 8.74 (d, J = 4.2 Hz, 1H), 8.33 (d, J = 6.3 Hz, 1H), 8.20 (dd, J = 8.0, 2.0 Hz, 1H), 7.84 (td, J = 7.9, 1.8 Hz, 1H), 7.41-7.34 (m, 2H), 7.29 (m, 1H). HRMS (ESI) m/z calcd for $C_{10}H_8N_2O$ ($[M+H]^+$) 173.0709, found 173.0625.

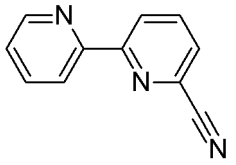

2,2'-Bipyridyl-6-Carbonitrile (*S-2*):

S-1 (3.635 g, 21.1 mmol) and trimethylsilylcyanide (6.60 mL, 52.6 mmol) were combined in a 50 mL round-bottomed flask with stir bar. Anhydrous CH_2Cl_2 (75 mL) was added to dissolve reagents, followed by placing the flask in an ice bath. Benzoyl chloride (2.45 mL, 21.1 mmol) was added slowly to this, followed by stirring at room temperature under a blanket of nitrogen. After five days all volatiles were evaporated *in vacuo*. The resulting solid was triturated with 1M aqueous NaOH (200 mL) and collected by filtration. The filter cake was then washed with 1M aqueous NaOH (50 mL) and deionized water (250 mL). The obtained dried off-white solid was determined to be spectroscopically pure product (2.438 g, 63%). ^{1}H NMR (400 MHz; $CDCl_3$) δ 8.70-8.65 (m, 2H), 8.46 (d, J = 8.0 Hz, 1H), 7.95 (t, J = 7.9 Hz, 1H), 7.85 (td, J = 7.8, 1.8 Hz, 1H), 7.70 (dd, J = 7.6, .9 Hz, 1H), 7.37 (ddd, J = 7.5, 4.8, 1.1 Hz, 1H). HRMS (ESI) m/z calcd for $C_{11}H_7N_3$ ($[M+H]^+$) 182.0712, found 182.0736.

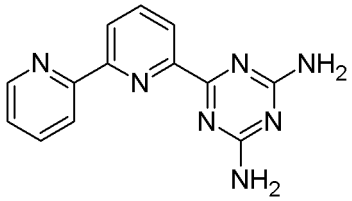

6-(3,5-Diamino-2,4,6-triazinyl)2,2'-bipyridine (1):

S-2 (248 mg, 1.37 mmol) was added to a 50 mL round-bottomed flask with stir bar, along with dicyandiamide (124 mg, 1.47 mmol) and KOH (34 mg, .61 mmol). A reflux condensor was attached, and iPrOH (20 mL) was added, followed by heating under reflux. After 18 h the reaction was cooled, and the precipitate was filtered. The filter cake was rinsed with iPrOH (120 mL) and deionized water (120 mL), then dried to give product as an off-white solid (259 mg, 71%). ^{1}H NMR (400 MHz; DMSO-d_6) δ 8.71(dd, J = 4.7, 0.7 Hz, 1H), 8.48 (d, J = 7.8 Hz, 2H), 8.20 (dd, J = 7.7, 0.9 Hz, 1H), 8.06 (td, J = 7.8 Hz, 1H), 7.98 (td, J = 7.7, 1.8 Hz, 1H), 7.48 (ddd, J = 7.4, 4.7, 1.0 Hz, 1H), 6.93 (br d, 4H). ^{13}C NMR (100 MHz; DMSO-d_6) δ 170.5, 167.6, 155.2, 155.0, 154.8, 149.3 (d, J = 6.4 Hz), 137.8, 137.2, 124.3, 123.6 (d, J = 6.5 Hz), 121.7 (d, J = 10.0Hz), 120.9 (d, J = 9.1 Hz). HRMS (ESI) m/z calcd for $C_{13}H_{11}N_7$ ($[M+H]^+$) 266.1148, found 266.1166.

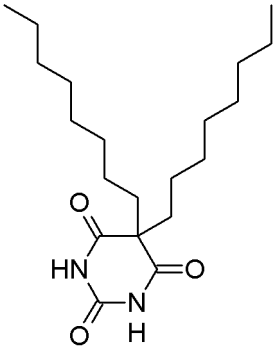

5,5-Dioctylbarbituric Acid (2):

Diethylmalonate (2.50 mL, 16.4 mmol) was slowly syringed into a 100 mL round-bottomed flask with stir bar containing anhydrous THF (50 mL), KI (260 mg, 1.57 mmol) and NaH suspended in mineral oil (1.36 g, 34.0 mmol). Once H_2 production ceased, 1-octylbromide (7.00 mL, 40.6 mmol) was added along with a reflux condensor, and reaction was purged using N_2, followed by heating under reflux. After 24 h, urea (990 mg, 16.5 mmol) was added, followed by slow addition of additional NaH suspended in mineral oil (1.34 g, 33.5 mmol). Reaction was then heated under reflux. After 24 h the reaction was cooled to room temperature, followed by

addition of 10% aqueous HCl to lower the pH to approximately 1. The volume was reduced *in vacuo* until all of the THF had been removed, giving rise to a precipitate. This was filtered and dried. The precipitate was then triturated in hexanes (100 mL), filtered, and rinsed with additional hexanes (100 mL). After drying, product was recovered as a faint-beige solid (1.25 g, 21%). ^{1}H NMR (400 MHz; $CDCl_3$) δ 8.71 (s, 2H), 1.96 (m, 4H), 1.22 (m, 24H), 0.87 (t, J = 6.8 Hz, 6H). ^{13}C NMR (100 MHz; $CDCl_3$) δ 178.0, 175.4, 58.0, 34.5, 32.0, 29.8, 29.3, 27.4, 24.6, 22.8, 14.2. HRMS (ESI) m/z calcd for $C_{20}H_{36}N_2O_3$ ($[M-H]^+$) 352.2642, found 351.2563.

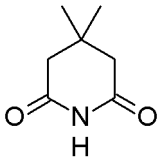

3,3-Dimethylglutarimide (3):

3,3-Dimethylglutaric anhydride (1.00 g, 7.03 mmol) and ammonium acetate (750 mg, 9.73 mmol) were combined in a 25 mL round-bottomed flask equipped with a reflux condenser. After purging with N_2 the mixture was heated to 155 °C. After 12 h the reaction was cooled. The solidified mixture was dissolved in CH_2Cl_2 (20 mL), followed by washing with deionized water (2 x 20 mL). The organic layer was dried over anhydrous $MgSO_4$ then evaporated *in vacuo* to give product as an off-white solid (717 mg, 71%). ^{1}H NMR (400 MHz; $CDCl_3$) δ 8.15 (br s, 1H), δ=2.44 (s, 4H), δ=1.12 (s, 6H). ^{13}C-NMR (100 MHz; $CDCl_3$) δ 172.2, 45.6, 30.6, 28.0. HRMS (ESI) m/z calcd for $C_7H_{11}NO_2$ ($[M+H]^+$) 142.0863, found 142.0866.

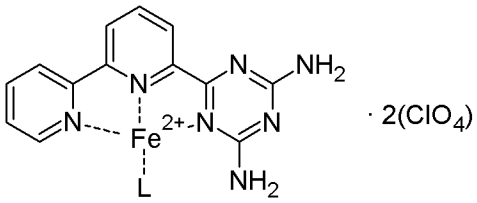

$(1)_2$•Fe•$(ClO_4)_2$:

1 (35.0 mg, .132 mmol) was added to a 25 mL round-bottomed flask and suspended in MeCN (10 mL). This was followed by addition of $Fe(ClO_4)_2 \cdot xH_2O$ (24.0 mg). Upon stirring the triazine began to dissolve and the solution took a deep purple color. After 5 minutes all of the triazine was observed to have dissolved, and the reaction mixture was diluted with Et_2O (240 mL), causing a purple precipitate to form. This was collected by vacuum filtration and dried *in vacuo* to give product as a purple powder (49.2 mg, 95%). ^{1}H NMR (400 MHz; DMSO-d_6) δ 19.79 (br s, 1H), 17.97 (br s, 1H), 15.61 (br s, 1H), 13.87 (br s, 1H), 9.23 (br s, 1H), 8.66 (br s, 1H), 8.24

(br s, 1H), 7.20 (br s, 1H); (400 MHz; CD_3CN) δ 25.27 (br s, 1H), 17.00 (br s, 1H), 15.41 (br s, 1H), 13.87 (br s, 1H), 12.03 (br s, 1H), 8.91 (t, J = 7.2 Hz, 1H), 7.90 (t, J = 7.3 Hz, 1H), 6.59 (br s, 1H), 5.75 (br s, 1H), 0.05 (br s, 2H); (400 MHz; Acetone-d_6) δ 19.21 (br s, 1H), 17.42 (br s, 1H), 15.40 (br s, 1H), 13.46 (br s, 1H), 9.21 (t, J = 7.0 Hz, 1H), 8.28 (t, J = 7.0 Hz, 1H), 7.67 (br s, 1H), 6.66 (br s, 1H); (400 MHz; D_2O) δ 14.41 (br s, 1H), 12.56 (br s, 1H), 11.85 (br s, 1H), 10.95 (br s, 1H), 9.23 (br s, 1H), 8.90 (t, J = 7.9 Hz, 1H), 7.81 (t, J = 7.6 Hz, 1H). HRMS (ESI) m/z calcd for $C_{26}H_{22}ClFeN_{14}O_4$ ($[M\text{-}ClO_4]^+$) 685.0981, found 685.0996.

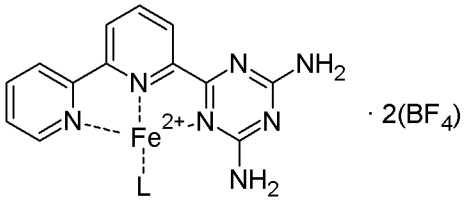

$(1)_2$•Fe•$(BF_4)_2$:

1 (2.0 mg, 7.5 μmol) was suspended in CD_3CN (500 μL) in an NMR tube. Meanwhile, $FeCl_2$ (11.5 mg, 91 μmol) and $AgBF_4$ (35.3 mg, 180 μmol) were combined in CD_3CN (1.0 mL), followed by vigorous shaking. After removal of AgCl by centrifugation, $Fe(BF_4)_2$ solution (42 μL, 3.8 μmol) was added to the tube, immediately causing the solution to turn purple. Sample was placed in an ultrasonification bath until no further residual solid was observed in the tube. ^1H NMR (400 MHz; CD_3CN) δ 25.76 (br s, 2H), 17.27 (br s, 1H), 15.61 (br s, 1H), 14.04 (br s, 1H), 12.19 (br s, 1H), 8.94 (br s, 1H), 7.93 (br s, 1H), 6.61 (br s, 1H), 5.77 (br s, 1H), 5.04 (br s, 2H).

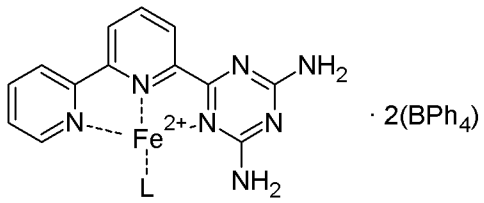

$(1)_2$•Fe•$(BPh_4)_2$:

1 (166 mg, 630 μmol) was suspended in CH_3CN (25 mL) along with $Fe(ClO_4)_2 \cdot xH_2O$ (114 mg) and sodium tetraphenylborate (214 mg, 630 μmol) in a 100 mL round-bottomed flask with star bar. This was stirred for ten minutes until all solids had dissolved, followed by dilution with deionized water (150 mL). The resulting fine precipitate was filtered through celite, followed by rinsing with additional deionized water (100 mL). The filter was then rinsed with Me_2CO (400 mL) to dissolve the precipitate. Removal of the solvent *in vacuo* gave product as a fluffy purple

solid (203 mg, 53%). ^{1}H NMR (400 MHz; DMSO) δ 17.52 (br s, 2H), 15.77 (br s, 2H), 14.18 (br s, 2H), 12.34 (br s, 2H), 8.91 (t, *J* = 7.5 Hz, 2H), 7.91 (t, *J* = 7.5 Hz, 2H), 7.27 (br s, 16H), 6.99 (t, *J* = 7.4 Hz, 16H), 6.83 (t, *J* = 7.1 Hz, 8H), 6.62 (br s, 2H), 5.75 (br s, 2H).

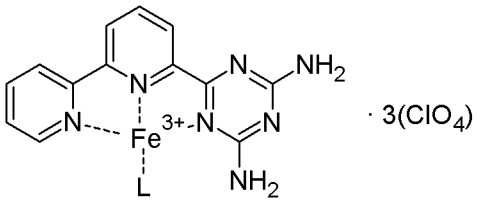

(1)$_2$•Fe•(ClO$_4$)$_3$:

1 (25.0 mg, 94 μmol) was suspended in CH_3CN (10 mL) along with $Fe(ClO_4)_3 \cdot xH_2O$ (23.0 mg) in a 25 mL round-bottomed flask with star bar. This was stirred for ten minutes until all solids had dissolved, followed by dilution with Et_2O (50 mL). The mixture was cooled to -25 °C, and the resulting precipitate was filtered through celite, followed by rinsing with addition Et_2O (25 mL). The filter was then rinsed with Me_2CO (100 mL) and MeCN (100 mL) to dissolve the precipitate. Removal of the solvent *in vacuo* gave product as an orange solid (38.5 mg, 92%). ^{1}H NMR (400 MHz; DMSO) δ 8.82 (d, *J* = 7.7 Hz, 1H), 8.70 (d, 0.3 Hz, 1H), 8.55 (d, *J* = 6.8 Hz, 1H), 8.47 (br s, 1H), 8.09 (m, 2H), 7.96 (t, *J* = 7.2 Hz, 1H), 7.74 (t, *J* = 4.3 Hz, 1H); (400 MHz; CD_3CN) δ 8.82 (d, *J* = 4.9 Hz, 1H), 8.66 (d, *J* = 8.1 Hz, 1H), 8.48 (m, 1H), 8.29 (d, *J* = 7.4 Hz, 1H), 8.20 (t, *J* = 7.8 Hz, 1H), 8.13 (br s, 1H), 7.84 (m, 1H), 6.44 (br s, 1H); (400 MHz; Acetone-d_6) δ 8.90 (d, *J* = 4.5 Hz, 1H), 8.85 (d, *J* = 8.0 Hz, 1H), 8.70 (d, *J* = 7.3 Hz, 1H), 8.48 (br s, 1H), 8.35 (t, *J* = 7.2 Hz, 1H), 8.26 (m, 2H), 7.82 (t, *J* = 5.6 Hz, 1H), 7.12 (br s, 1H).

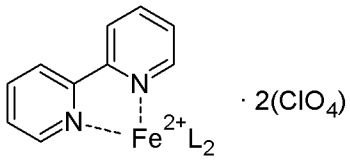

(Bipy)$_3$• Fe•(ClO$_4$)$_2$:

2,2'-Bipyridine (39.5 mg, 253 μmol) was added to an NMR tube. $Fe(ClO_4)_2 \cdot xH_2O$ (58.9 mg) was dissolved in DMSO-d_6 (1.0 mL), and 520 μL of this solution were added to the NMR tube, causing an immediate color change to a deep red. The sample was sonicated until no further residual solid was observed in the tube. ^{1}H NMR (400 MHz; DMSO-d_6) δ 8.84 (d, *J* = 7.8 Hz, 2H), 8.22 (t, *J* = 7.4 Hz, 2H), 7.54 (t, *J* = 6.0 Hz, 2H), 7.42 (d, *J* = 4.9 Hz, 2H); ^{13}C NMR (100 MHz; DMSO-d_6) δ 158.8, 153.7, 138.8, 127.7, 124.1.

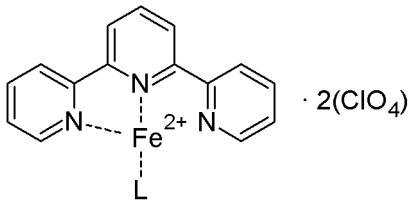

$(Terpy)_2$• Fe•$(ClO_4)_2$:

2,2';6',2''-Terpyridine (2.2 mg, 9.4 µmol) was added to an NMR tube along with DMSO-d_6 (480 µL). $Fe(ClO_4)_2 \cdot xH_2O$ (58.9 mg) was dissolved in DMSO-d_6, and 20 µL of this solution were added to the NMR tube, causing an immediate color change to a deep purple. The sample was sonicated until no further residual solid was observed in the tube. ^{1}H-NMR (400 MHz; DMSO-d_6) δ 9.25 (d, J = 8.0 Hz, 2H), 8.82 (m, 2H), 7.99 (t, J = 7.7 Hz, 2H), 7.18 (t, J = 6.5 Hz, 2H), 7.13 (d, J = 5.1 Hz, 2H).

3. NMR Spectra of Synthesized Compounds

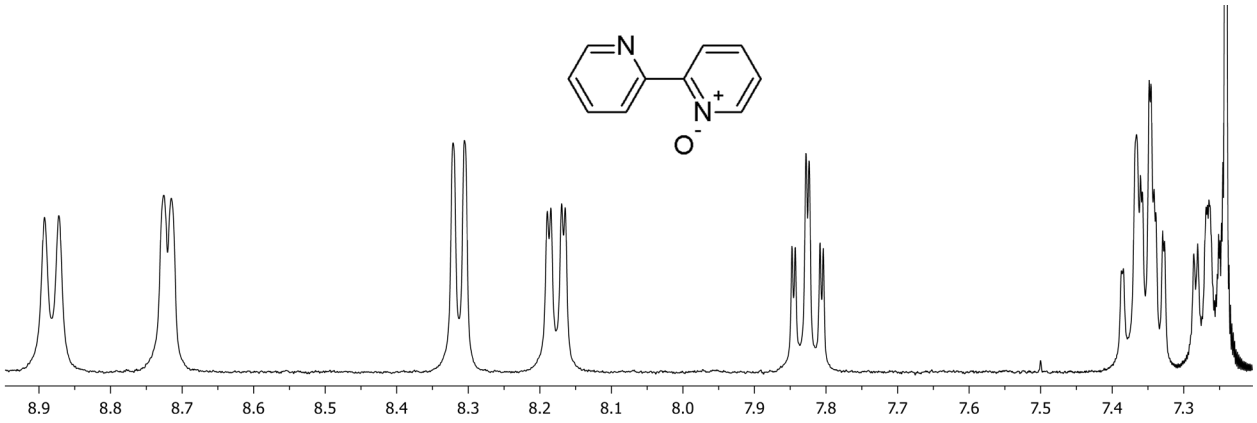

Figure S-1. ^{1}H NMR spectrum of ***S-1*** ($CDCl_3$, 400 MHz, 298 K).

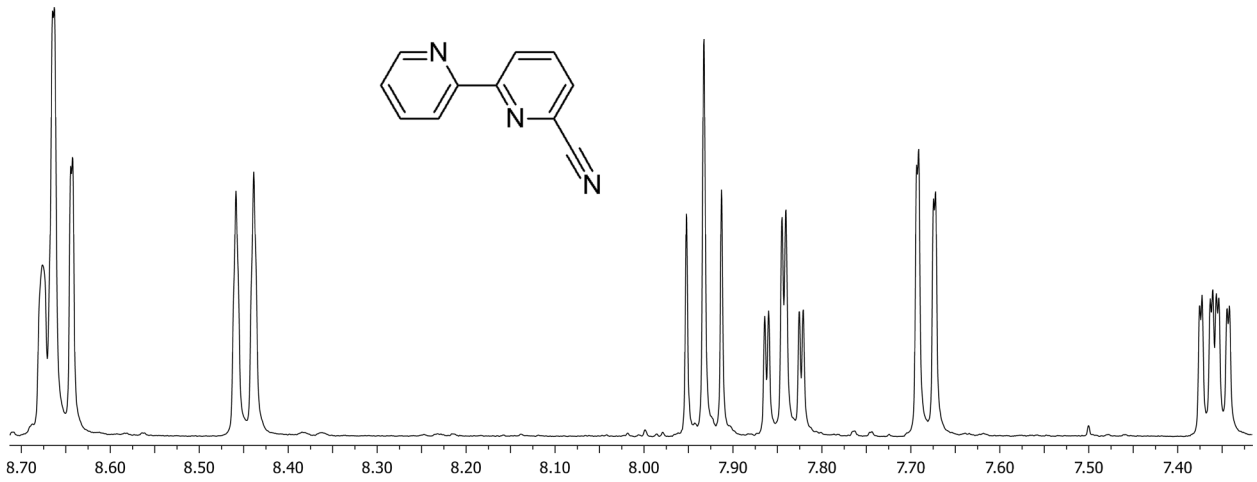

Figure S-2. ^{1}H NMR spectrum of ***S-2*** ($CDCl_3$, 400 MHz, 298 K).

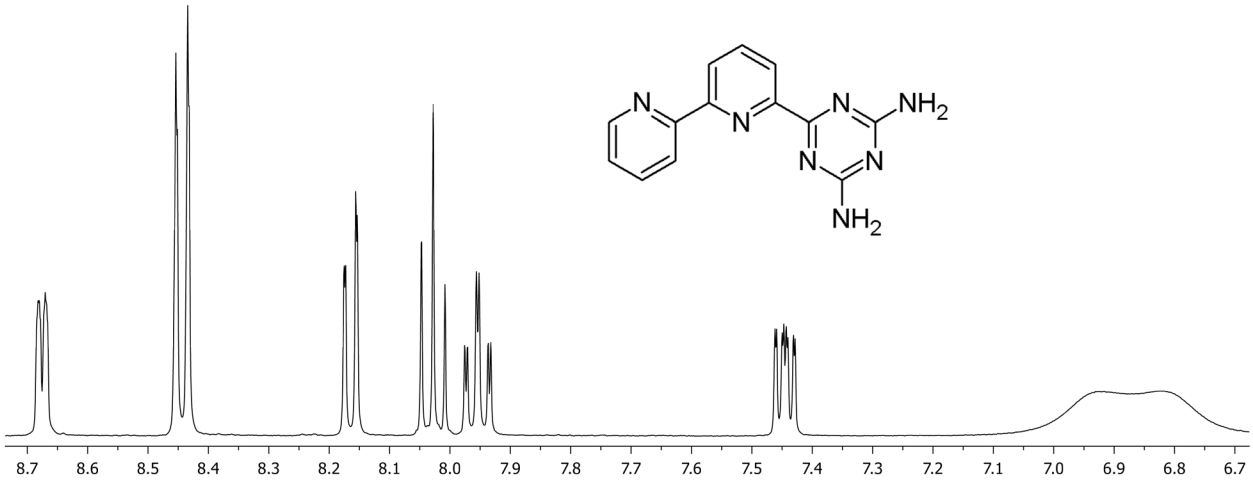

Figure S-3. ^{1}H NMR spectrum of **1** (DMSO-d_6, 400 MHz, 298 K).

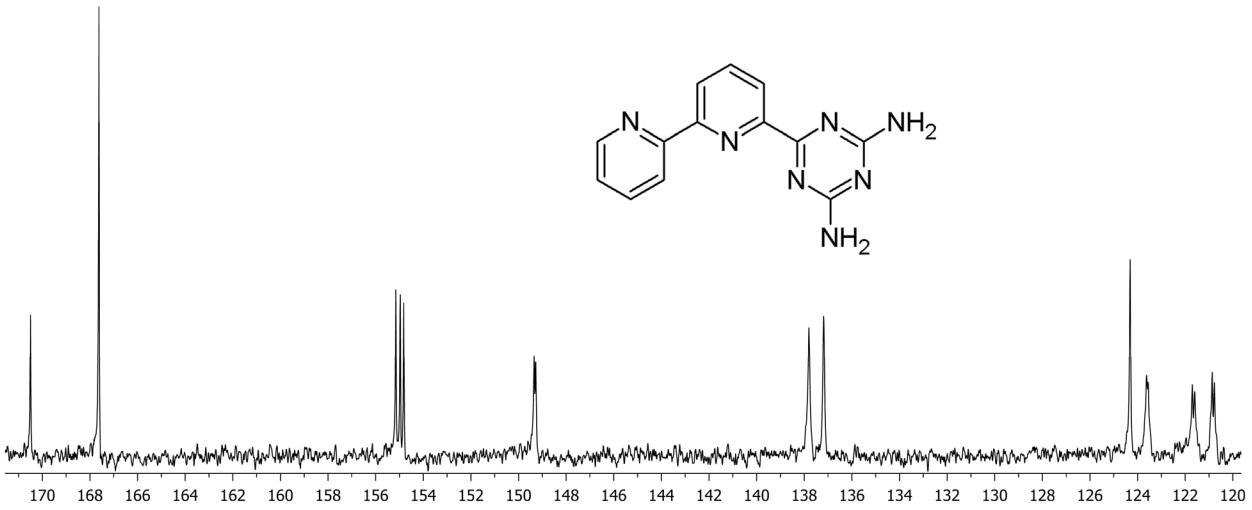

Figure S-4. ^{13}C NMR spectrum of **1** (DMSO-d_6, 100 MHz, 298 K).

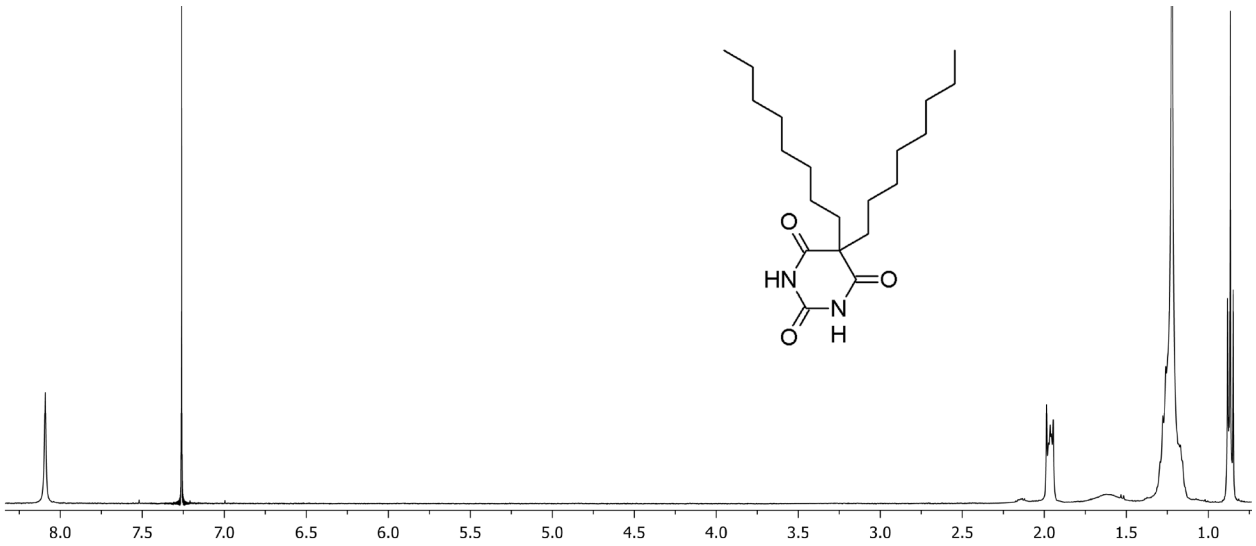

Figure S-5. ^{1}H NMR spectrum of **2** ($CDCl_3$, 400 MHz, 298 K).

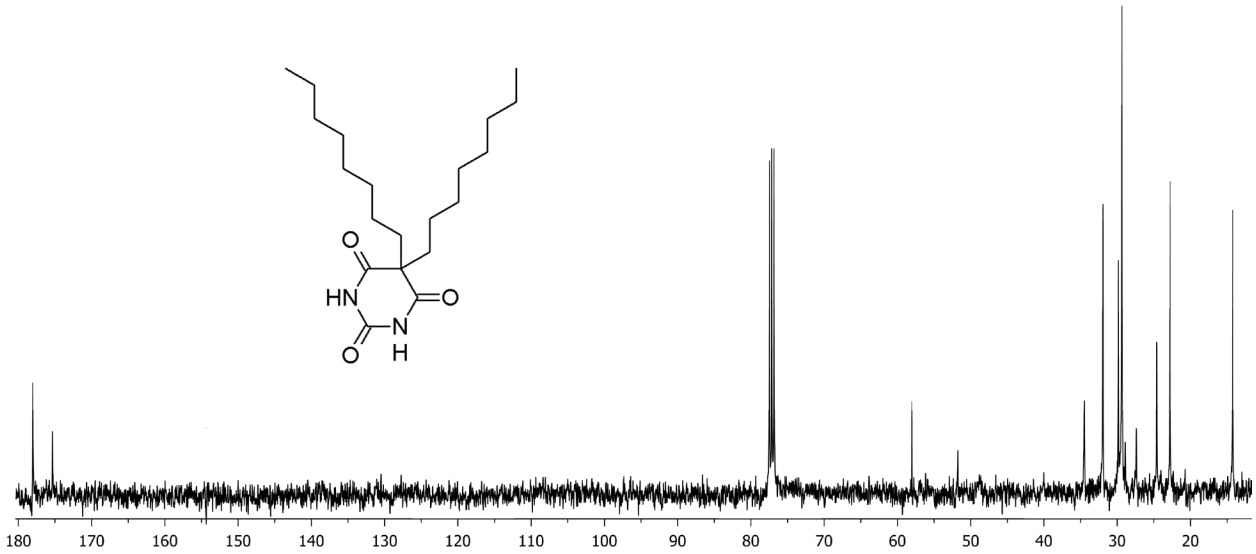

Figure S-6. ^{13}C NMR spectrum of **2** ($CDCl_3$, 400 MHz, 298 K).

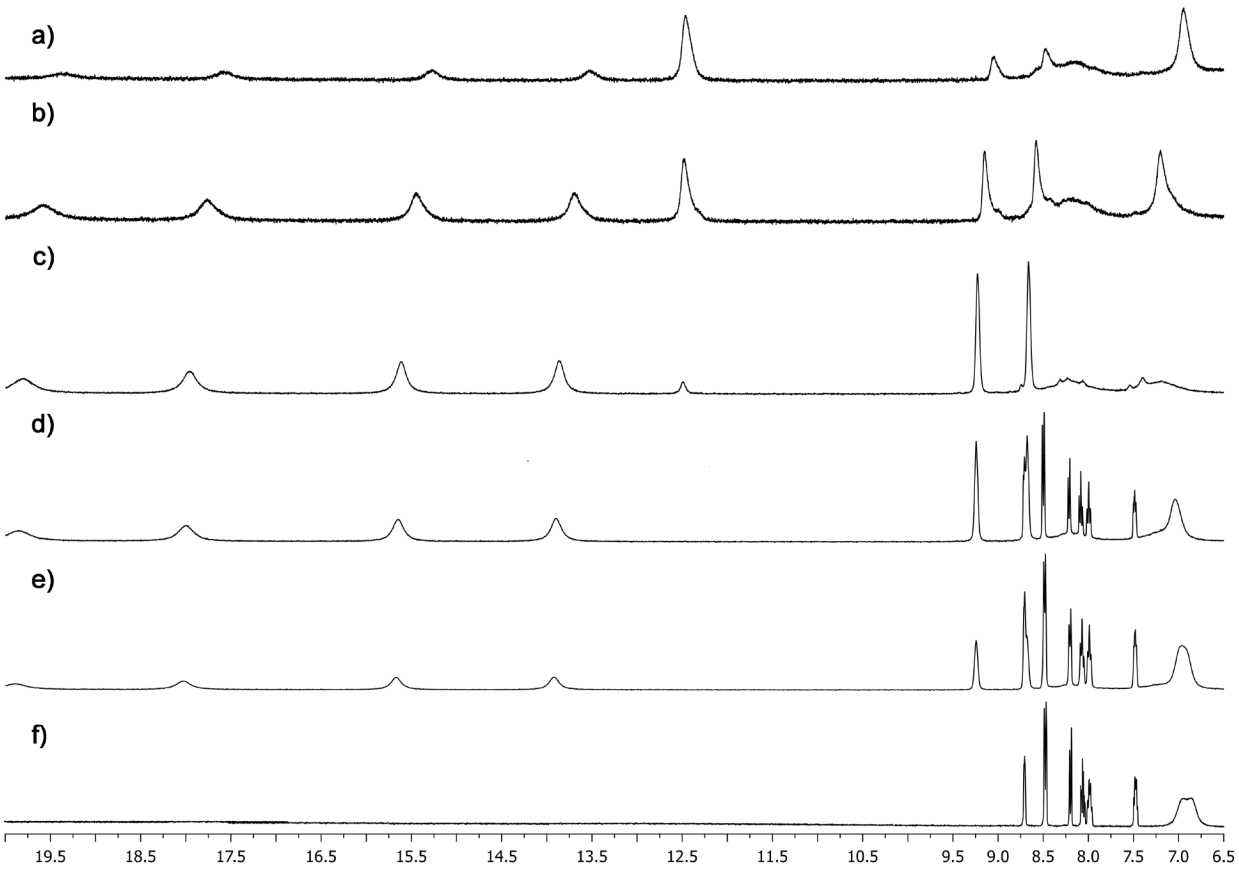

Figure S-7. ^{1}H NMR spectrum of the titration of $Fe(ClO_4)_2 \cdot xH_2O$ into a solution of **1** (DMSO-d_6, 400 MHz, 298 K): a) 1.0 eq $Fe(ClO_4)_2$; b) 0.66 eq $Fe(ClO_4)_2$; c) 0.5 eq $Fe(ClO_4)_2$; d) 0.33 eq $Fe(ClO_4)_2$; e) 0.25 eq $Fe(ClO_4)_2$; f) 0 eq $Fe(ClO_4)_2$.

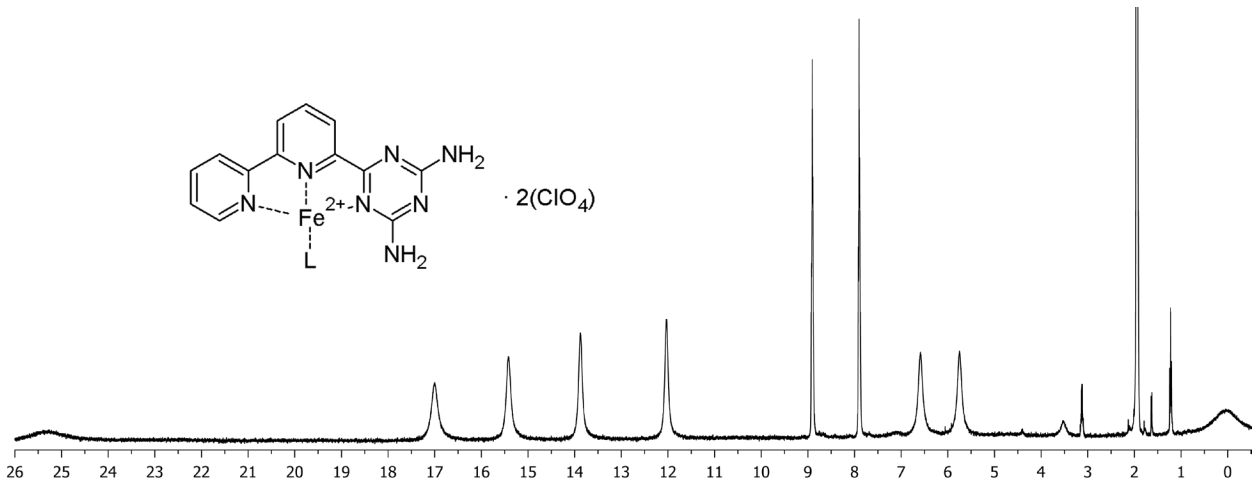

Figure S-8. ^{1}H NMR spectrum of $(\mathbf{1})_2$•Fe•$(ClO_4)_2$ (CD_3CN, 400 MHz, 298 K).

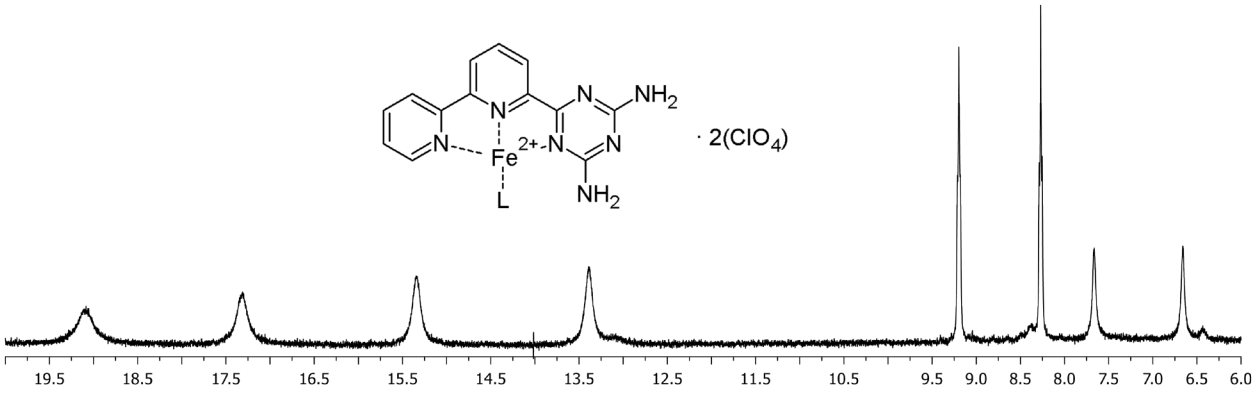

Figure S-9. ^{1}H NMR spectrum of (**1**)$_2$•Fe•(ClO$_4$)$_2$ (Acetone-d_6, 400 MHz, 298 K).

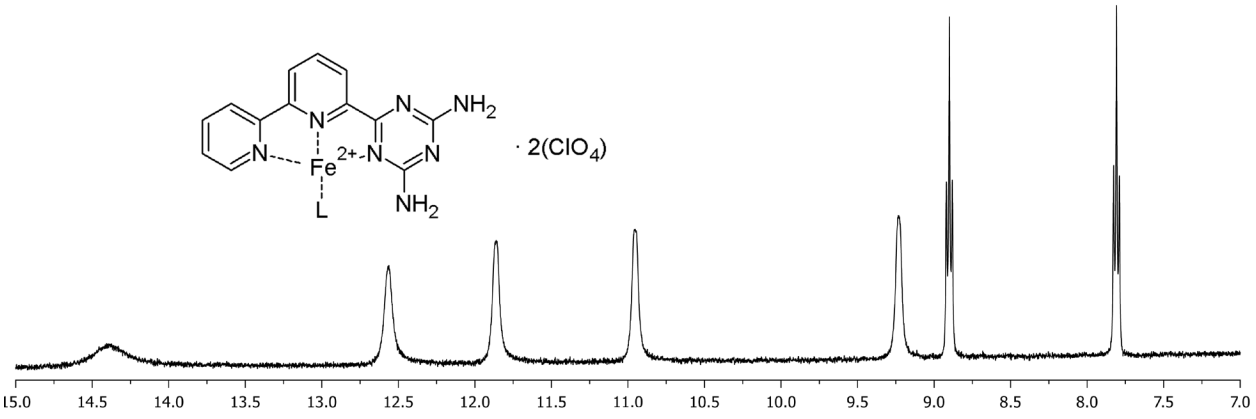

Figure S-10. ^{1}H NMR spectrum of (**1**)$_2$•Fe•(ClO$_4$)$_2$ (D$_2$O, 400 MHz, 298 K).

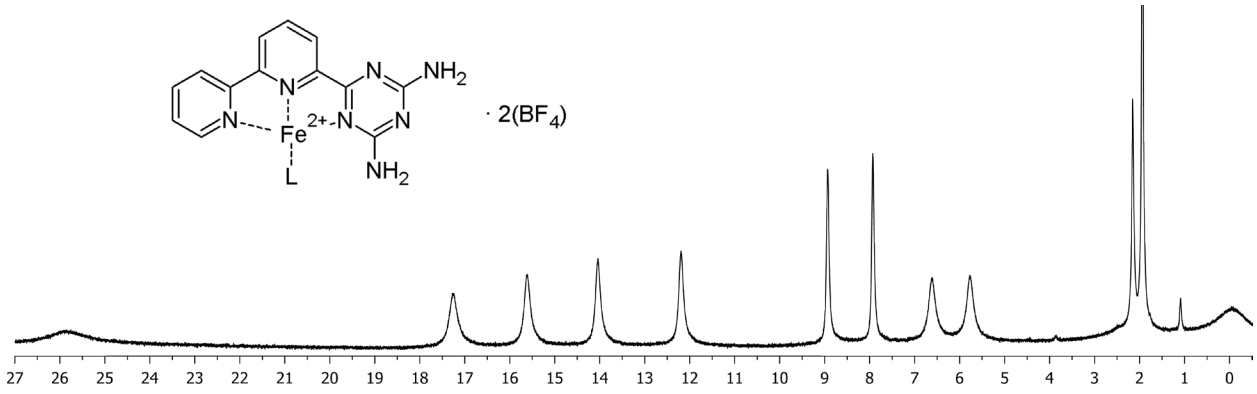

Figure S-11. ^{1}H NMR spectrum of $(\mathbf{1})_2$•Fe•$(BF_4)_2$ (CD_3CN, 400 MHz, 298 K).

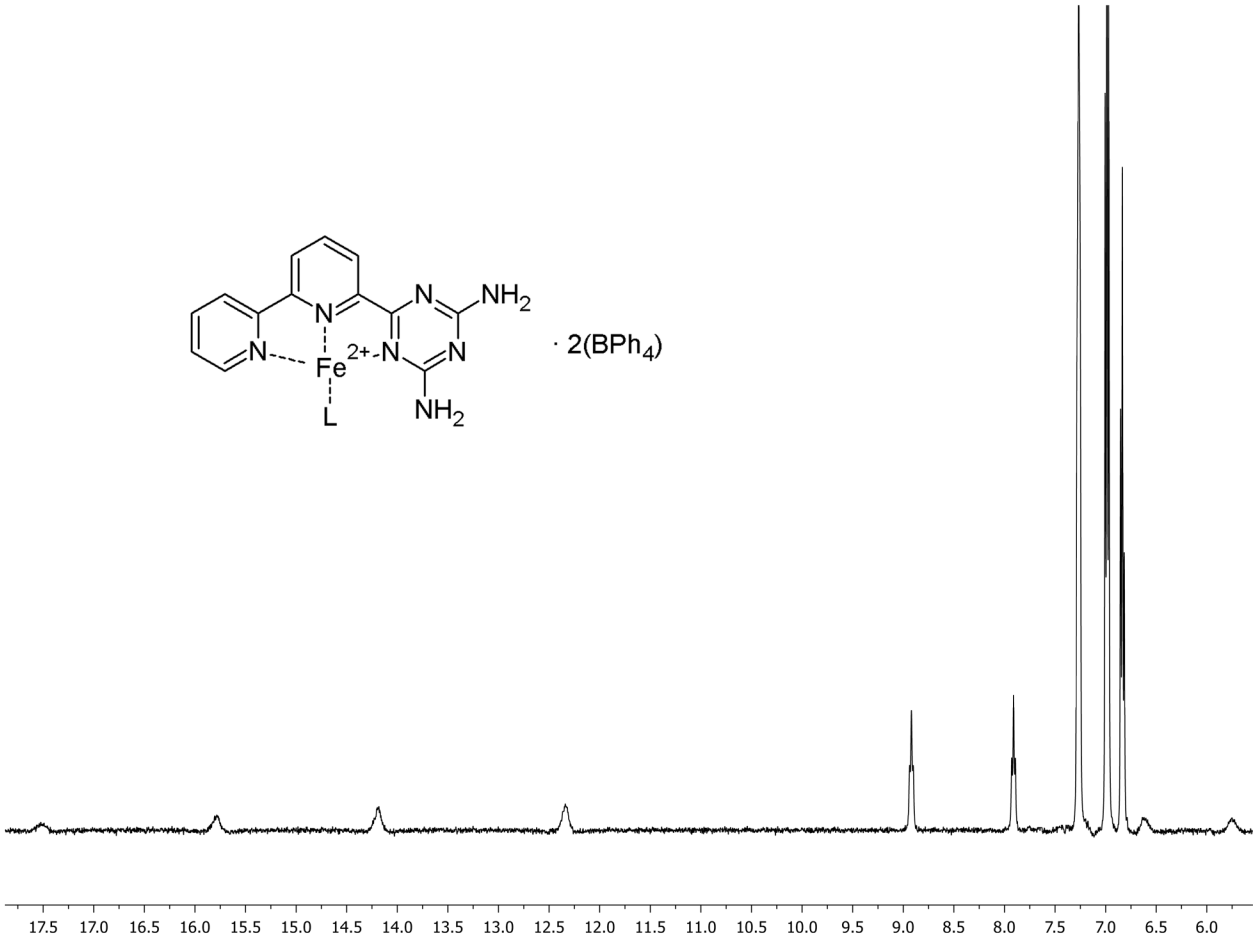

Figure S-12. ^{1}H NMR spectrum of $(\mathbf{1})_2$•Fe•$(BPh_4)_2$ (CD_3CN, 400 MHz, 298 K).

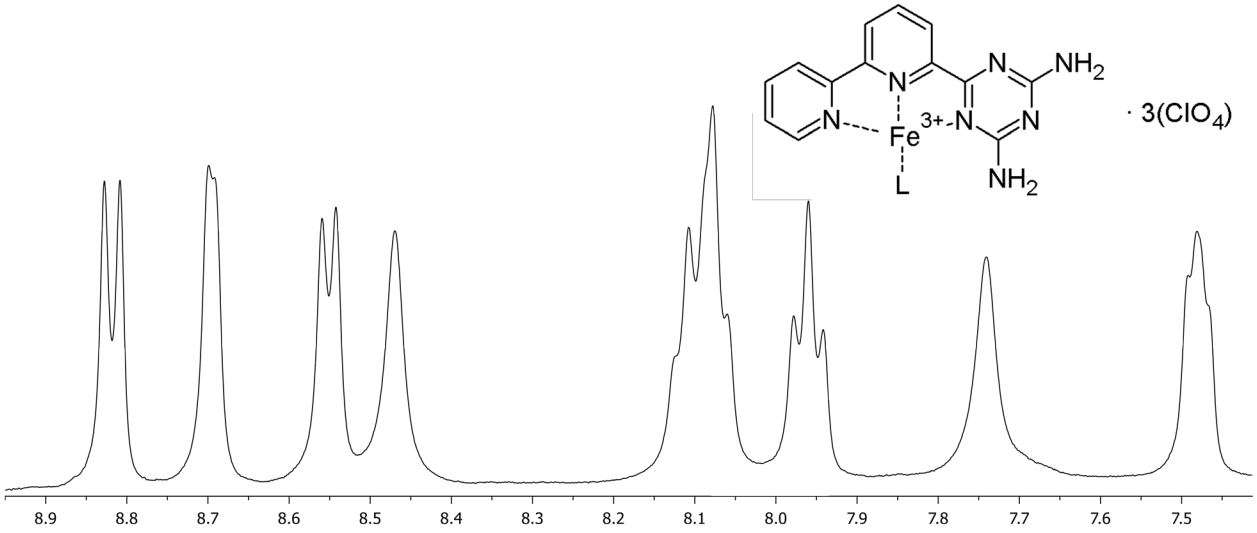

Figure S-13. ^{1}H NMR spectrum of $(\mathbf{1})_2$•Fe•$(ClO_4)_3$ (DMSO-d_6, 400 MHz, 298 K).

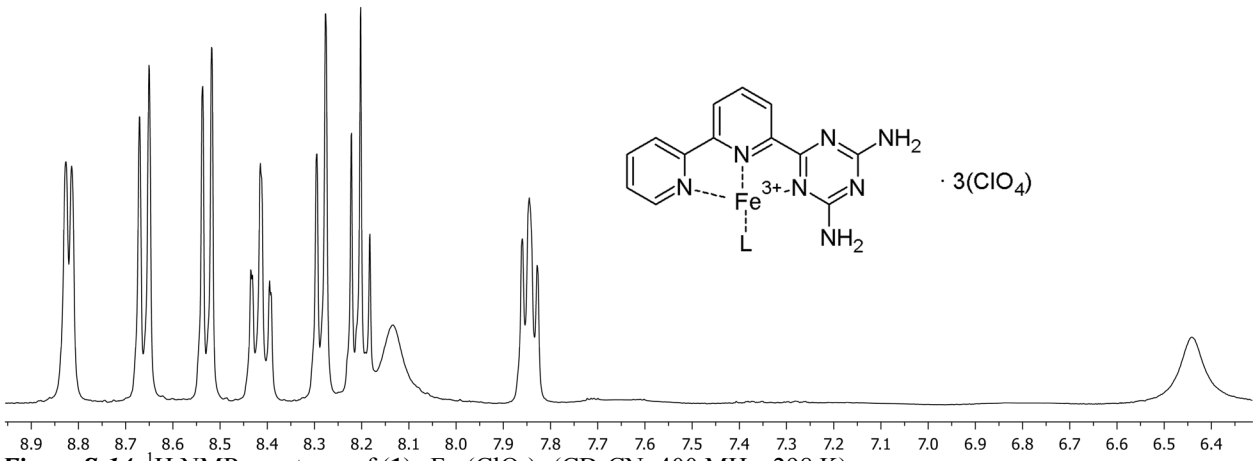

Figure S-14. ^{1}H NMR spectrum of $(\mathbf{1})_2$•Fe•$(ClO_4)_3$ (CD_3CN, 400 MHz, 298 K).

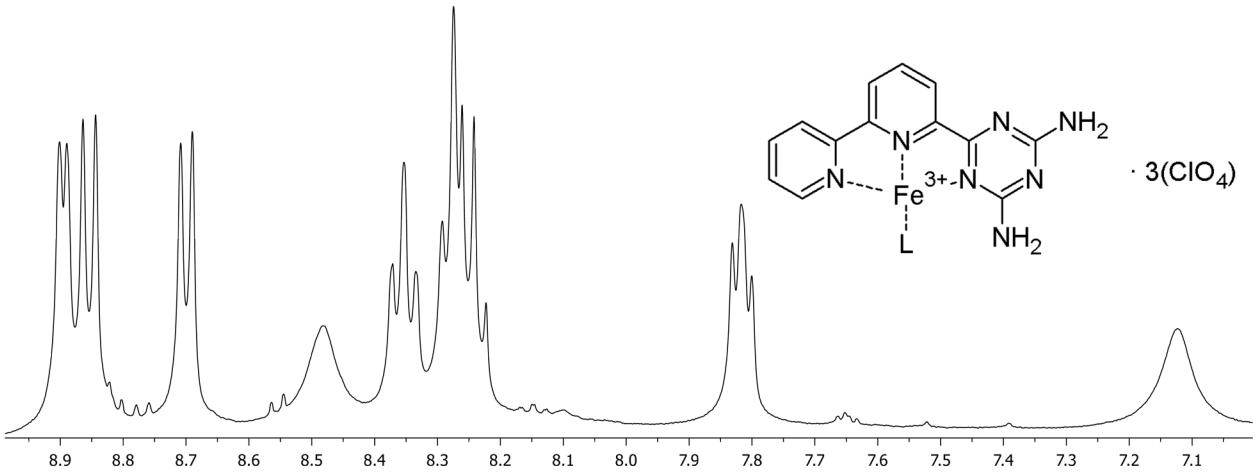

Figure S-15. ^{1}H NMR spectrum of (**1**)$_2$•Fe•(ClO$_4$)$_3$ (Acetone-d_6, 400 MHz, 298 K).

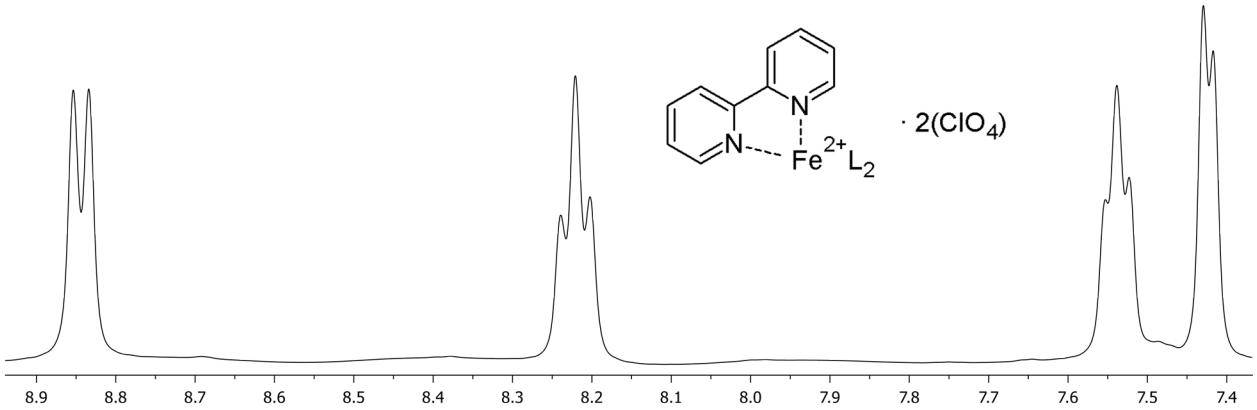

Figure S-16. ^{1}H NMR spectrum of (Bipy)$_3$• Fe•(ClO$_4$)$_2$ (DMSO-d_6, 400 MHz, 298 K).

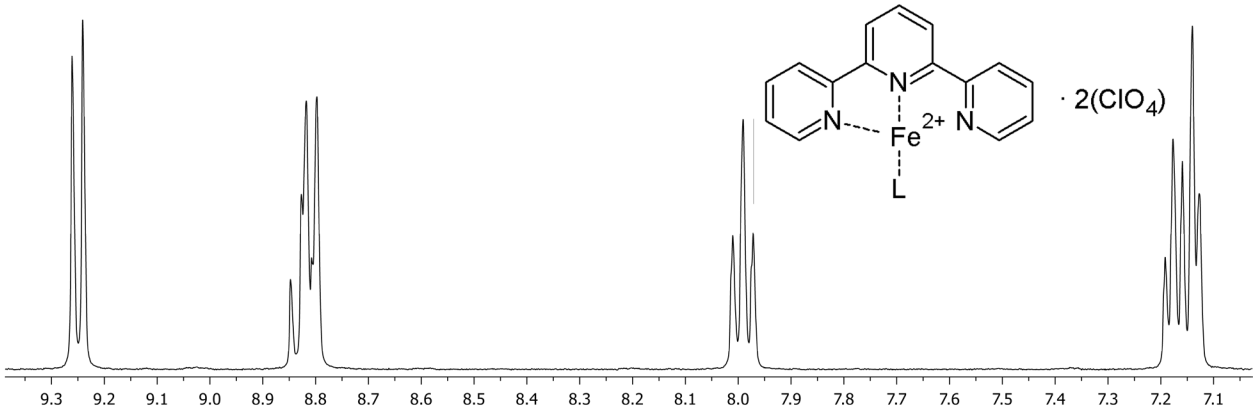

Figure S-17. ^{1}H NMR spectrum of (Terpy)$_2$• Fe•(ClO$_4$)$_2$ (DMSO-d_6, 400 MHz, 298 K).

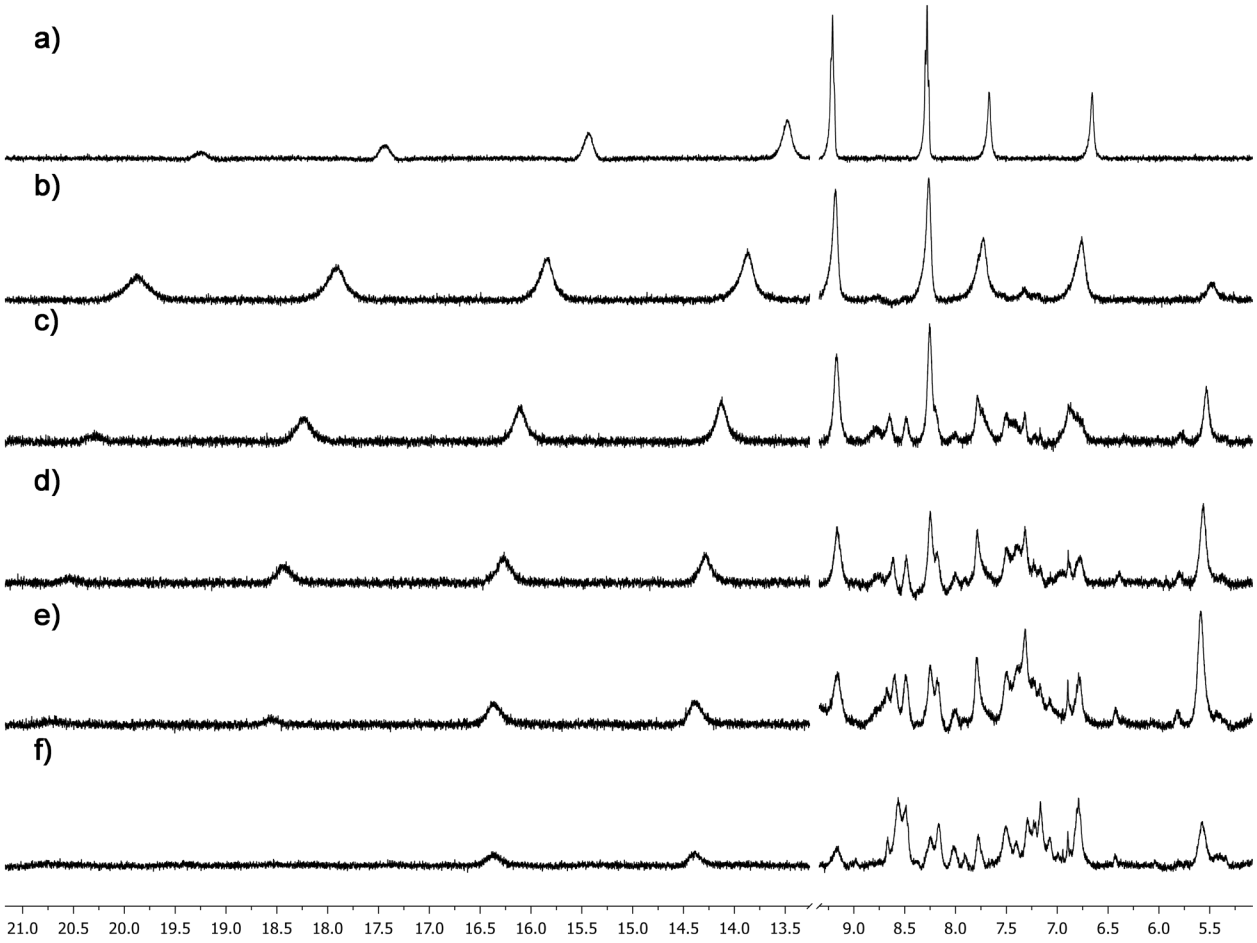

Figure S-18. ^{1}H NMR titration of **2** into (**1**)$_2$• Fe•$(ClO_4)_2$: a) 0 eq **2**; b) 22.5 eq **2**; c) 46 eq **2**; d) 68.5 eq **2**; e) 91.3 eq **2**; f) 114 eq **2** (Acetone-d_6, 500 MHz, 1.9 x 10^{-3} M, 298 K).

4. UV/Vis Spectra

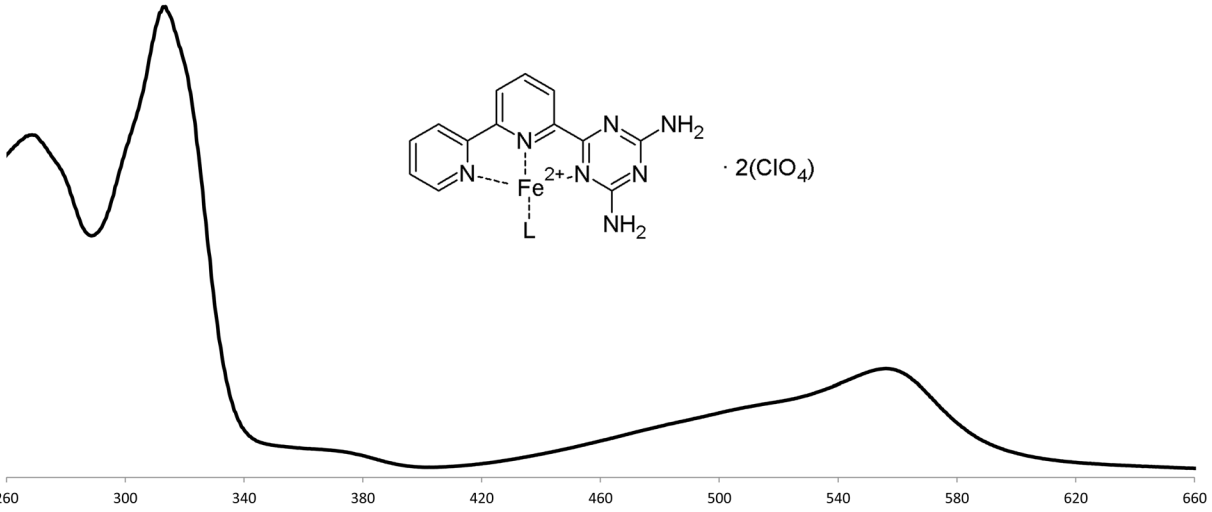

Figure S-19. UV/Vis spectrum of $(\mathbf{1})_2$•Fe•$(ClO_4)_2$ (MeCN, 7.5 x 10^{-5} M).

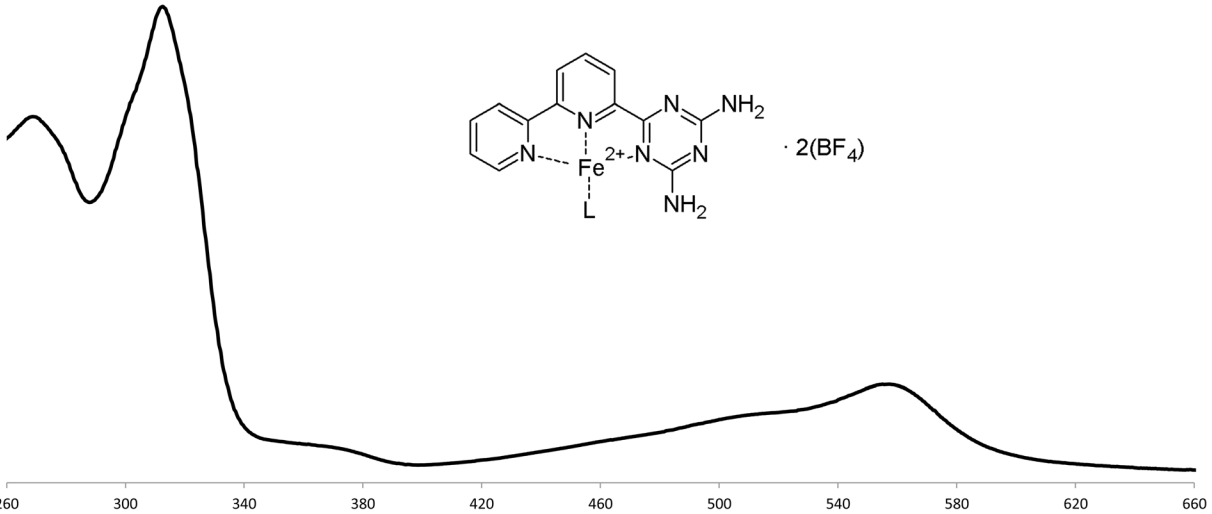

Figure S-20. UV/Vis spectrum of $(\mathbf{1})_2$•Fe•$(BF_4)_2$ (MeCN, 3.9 x 10^{-5} M).

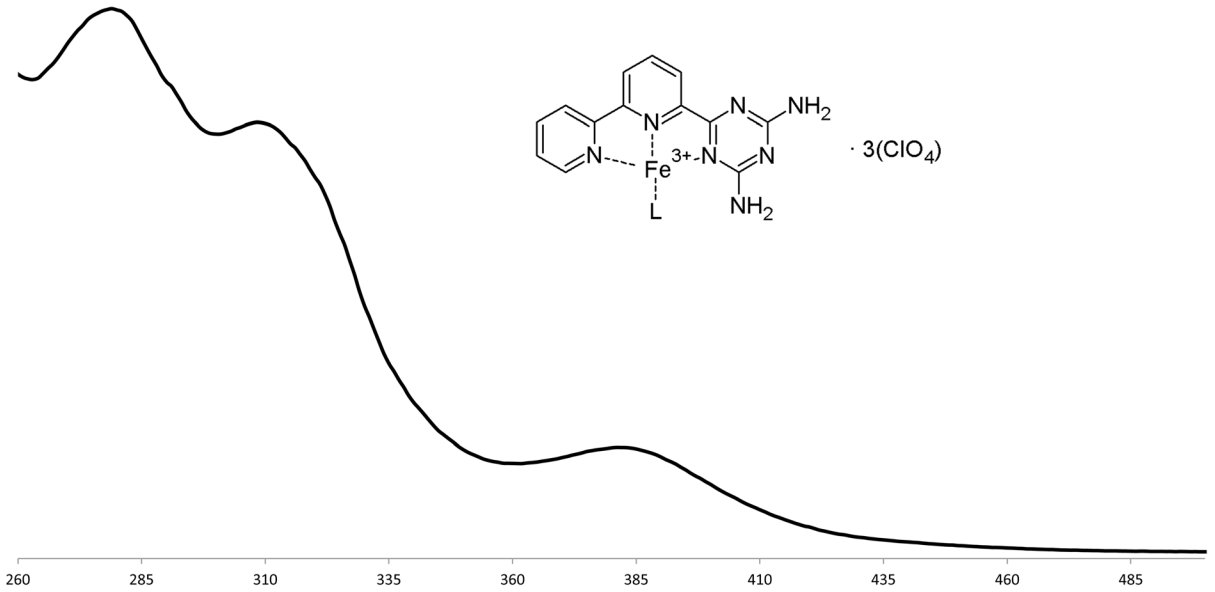

Figure S-21. UV/Vis spectrum of $(\mathbf{1})_2$•Fe•$(ClO_4)_3$ (MeCN, 3.8 x 10^{-5} M).

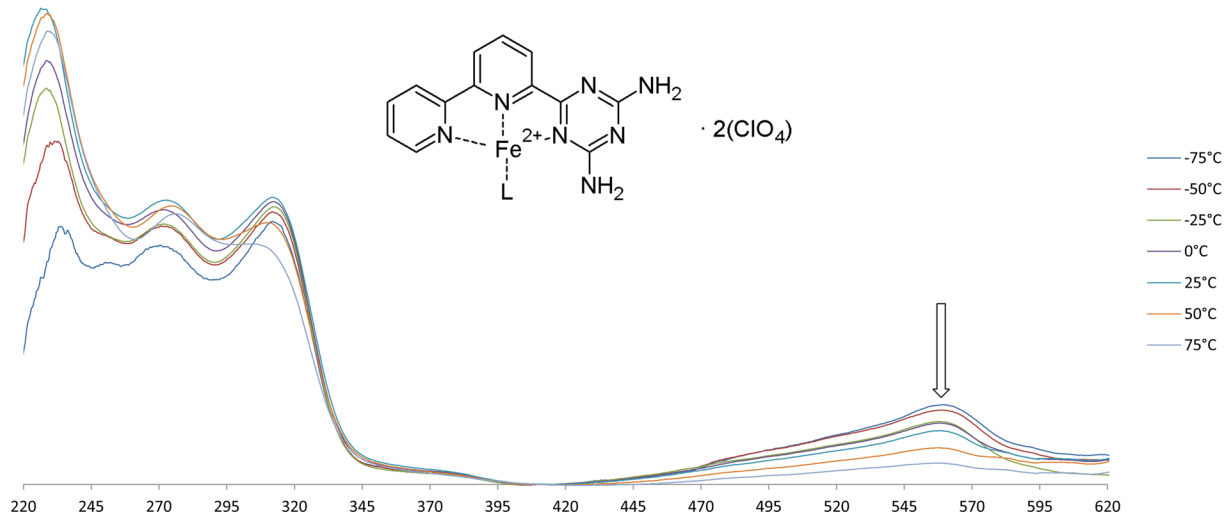

Figure S-22. Variable Temperature UV/Vis spectra of $(\mathbf{1})_2$•Fe•$(ClO_4)_2$ (EtOH, 2.9 x 10^{-5} M).

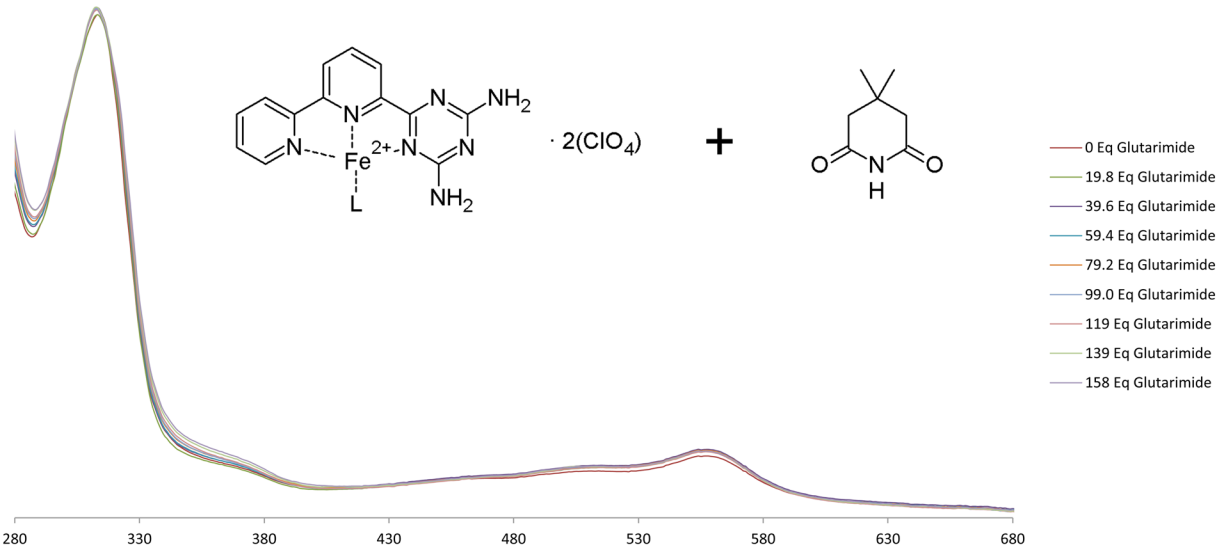

Figure S-23. UV/Vis spectra of **3** titrated into $(\mathbf{1})_2$•Fe•$(ClO_4)_2$ (MeCN, 2.6 x 10^{-5} M).

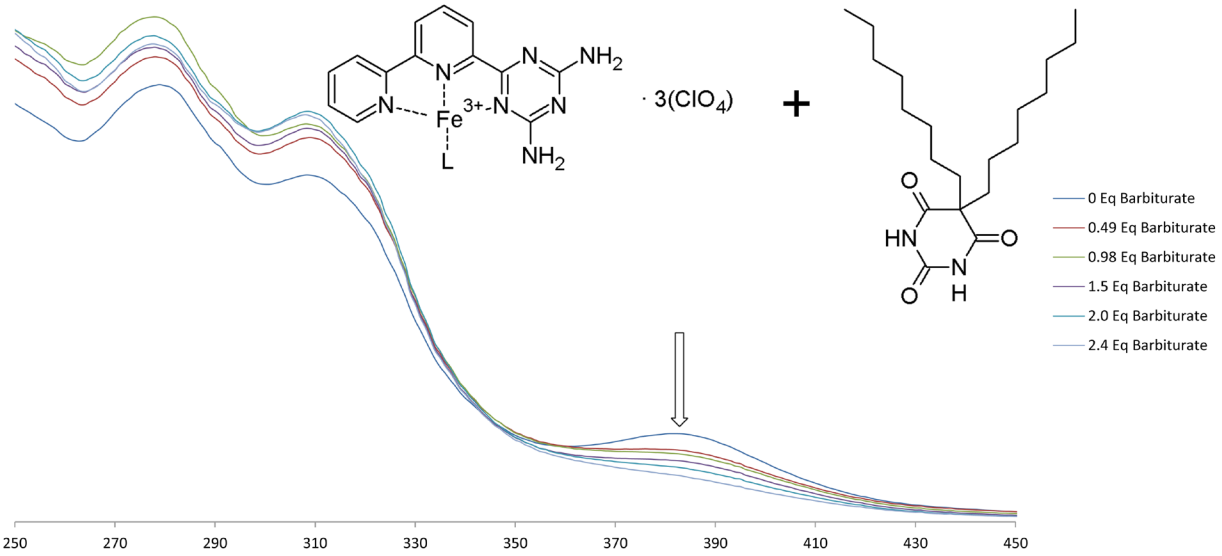

Figure S-24. UV/Vis spectra of **2** titrated into $(\mathbf{1})_2$•Fe•$(ClO_4)_3$ (MeCN, 2.6 x 10^{-5} M).

5. Cyclic Voltammetry

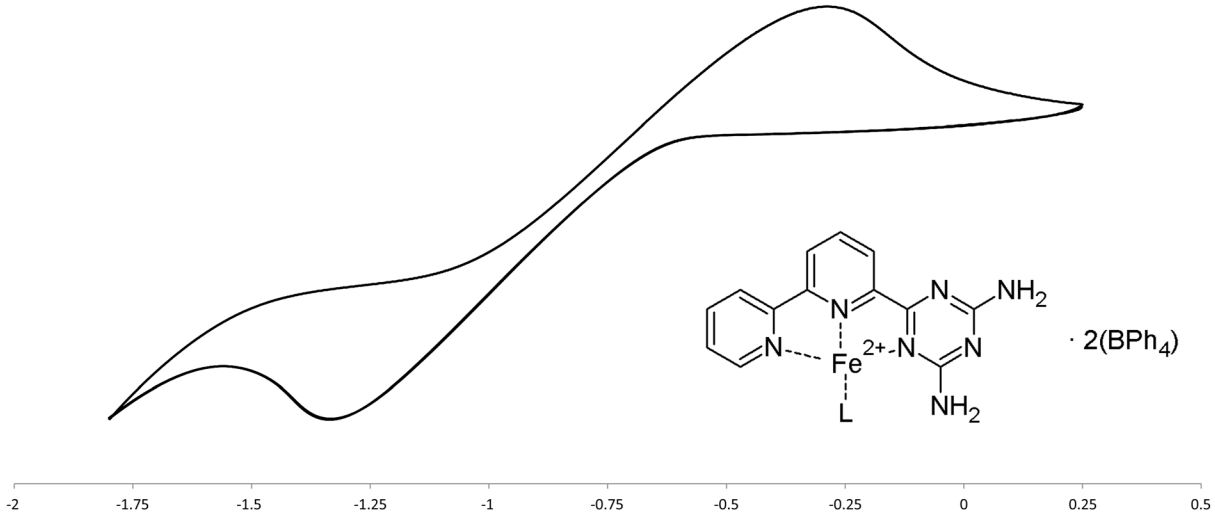

Figure S-25. Cyclic voltammogram of $(\mathbf{1})_2$•Fe•$(BPh_4)_2$ (MeCN, 500 µM Bu_4NBF_4 Buffer, 4.8 x 10^{-5} M, Scan Rate = 0.05 V/s).

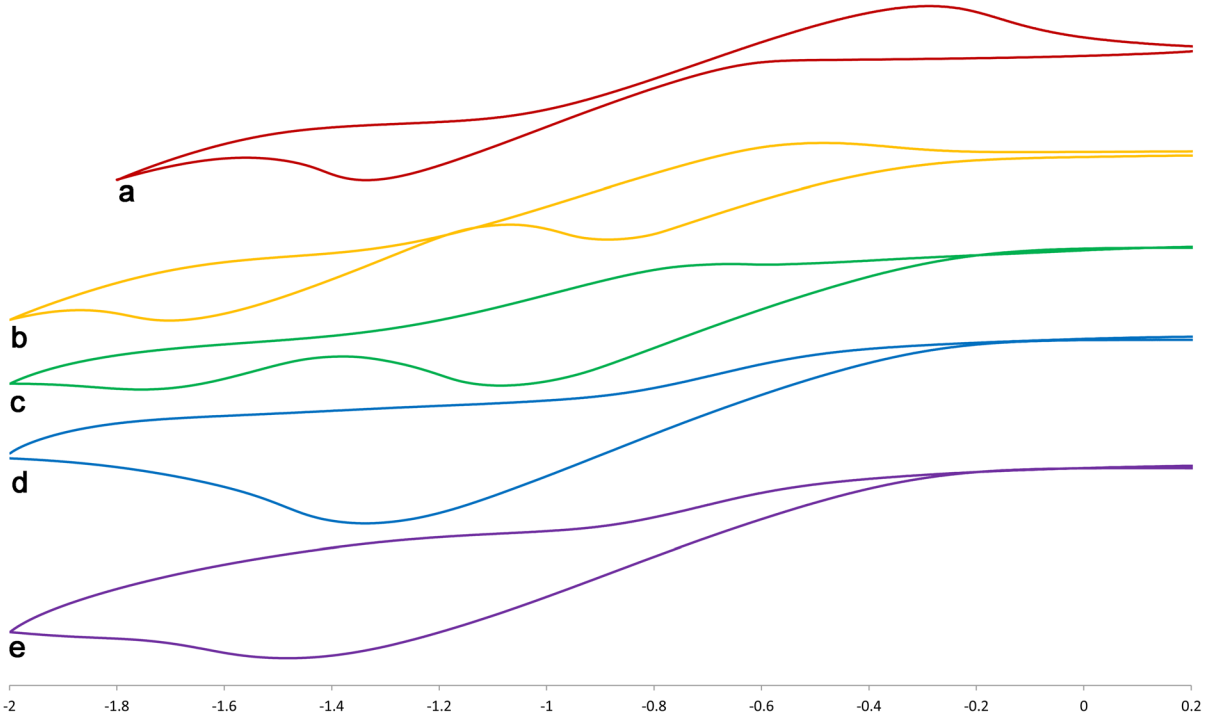

Figure S-26. Cyclic voltammogram of $(\mathbf{1})_2$•Fe•$(BPh_4)_2$ (MeCN, 500 µM Bu_4NBF_4 Buffer, 4.8 x 10^{-5} M, Scan Rate = 0.05 V/s): a) 0 eq Barbiturate; b) 44 eq Barbiturate; c) 89 eq Barbiturate; d) 133 eq Barbiturate; e) 177 eq Barbiturate.

6. Data Tables

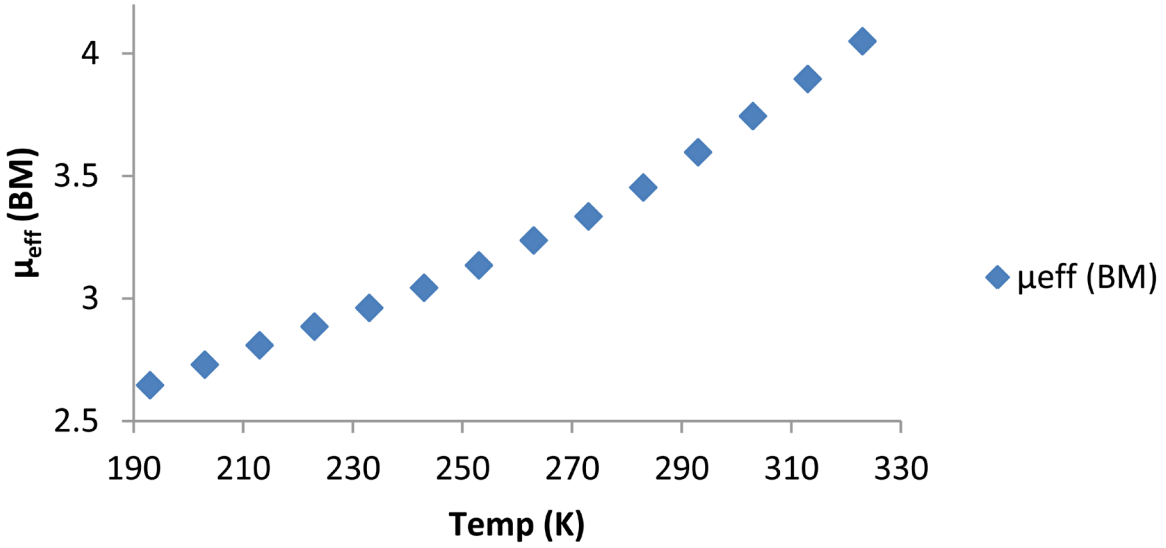

Figure S-27. Effective spin of $(\mathbf{1})_2$•Fe•$(ClO_4)_2$ calculated by the Evans Method[1] as a function of temperature (Acetone-d_6, 500 MHz, 8.24 x 10^{-3} M).

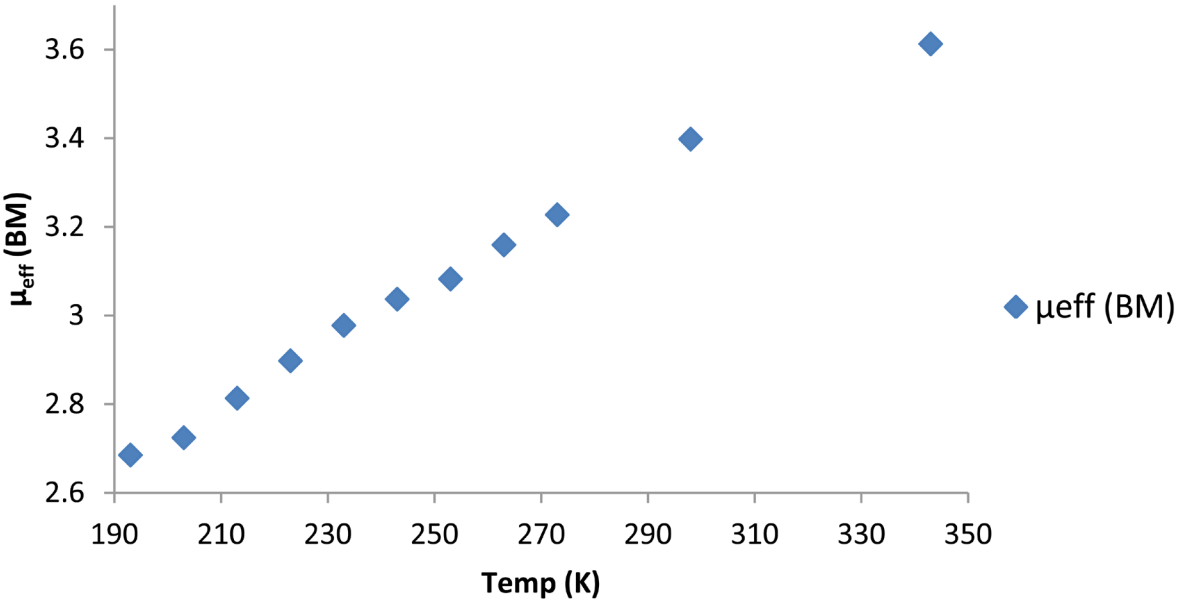

Figure S-28. Effective spin of $(\mathbf{1})_2$•Fe•$(ClO_4)_3$ calculated by the Evans Method[1] as a function of temperature (Acetone-d_6, 500 MHz, 1.92 x 10^{-2} M).

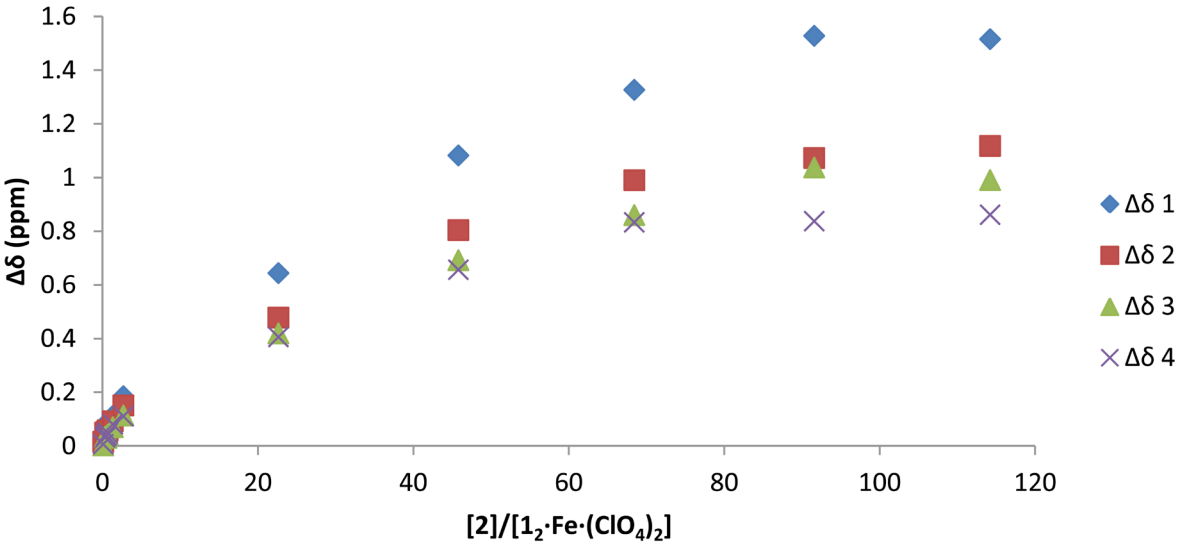

Figure S-29. Changes in chemical shift of selected proton resonances (19.21, 17.42, 15.40, and 13.46 ppm in the initial spectrum) of $(\mathbf{1})_2$•Fe•$(ClO_4)_2$ as a function of the concentration of **2** (Acetone-d_6, 500 MHz, 1.90 x 10^{-3} M).

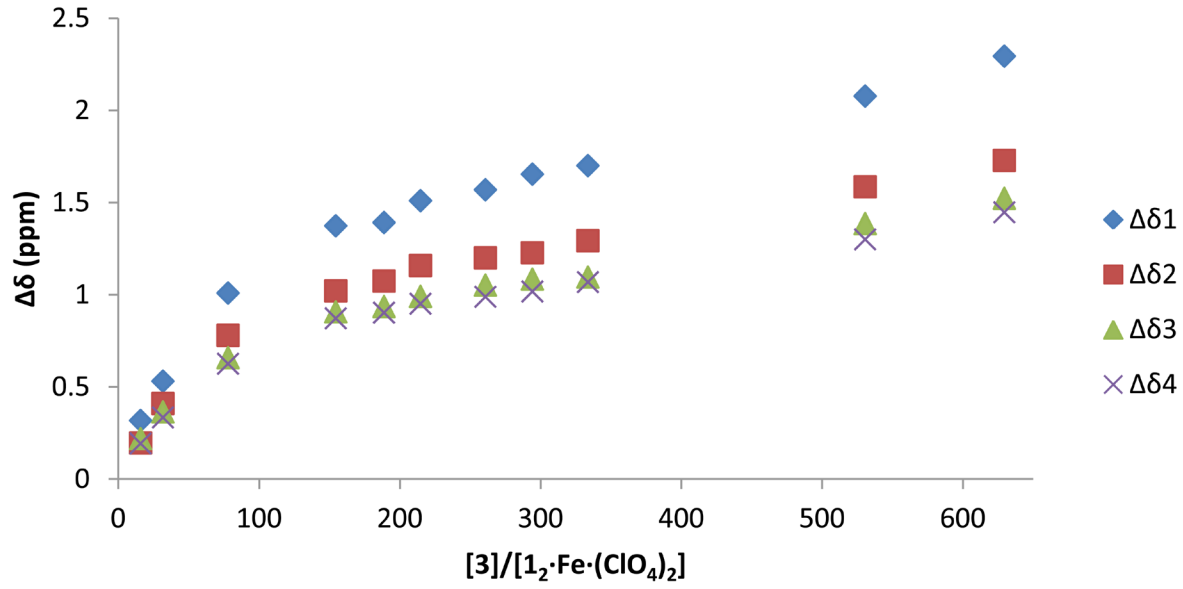

Figure S-30. Changes in chemical shift of selected proton resonances (19.21, 17.42, 15.40, and 13.46 ppm in the initial spectrum) of $(\mathbf{1})_2$•Fe•$(ClO_4)_2$ as a function of the concentration of **3** (Acetone-d_6, 500 MHz, 3.29 x 10^{-3} M).

7. Molecular Modeling

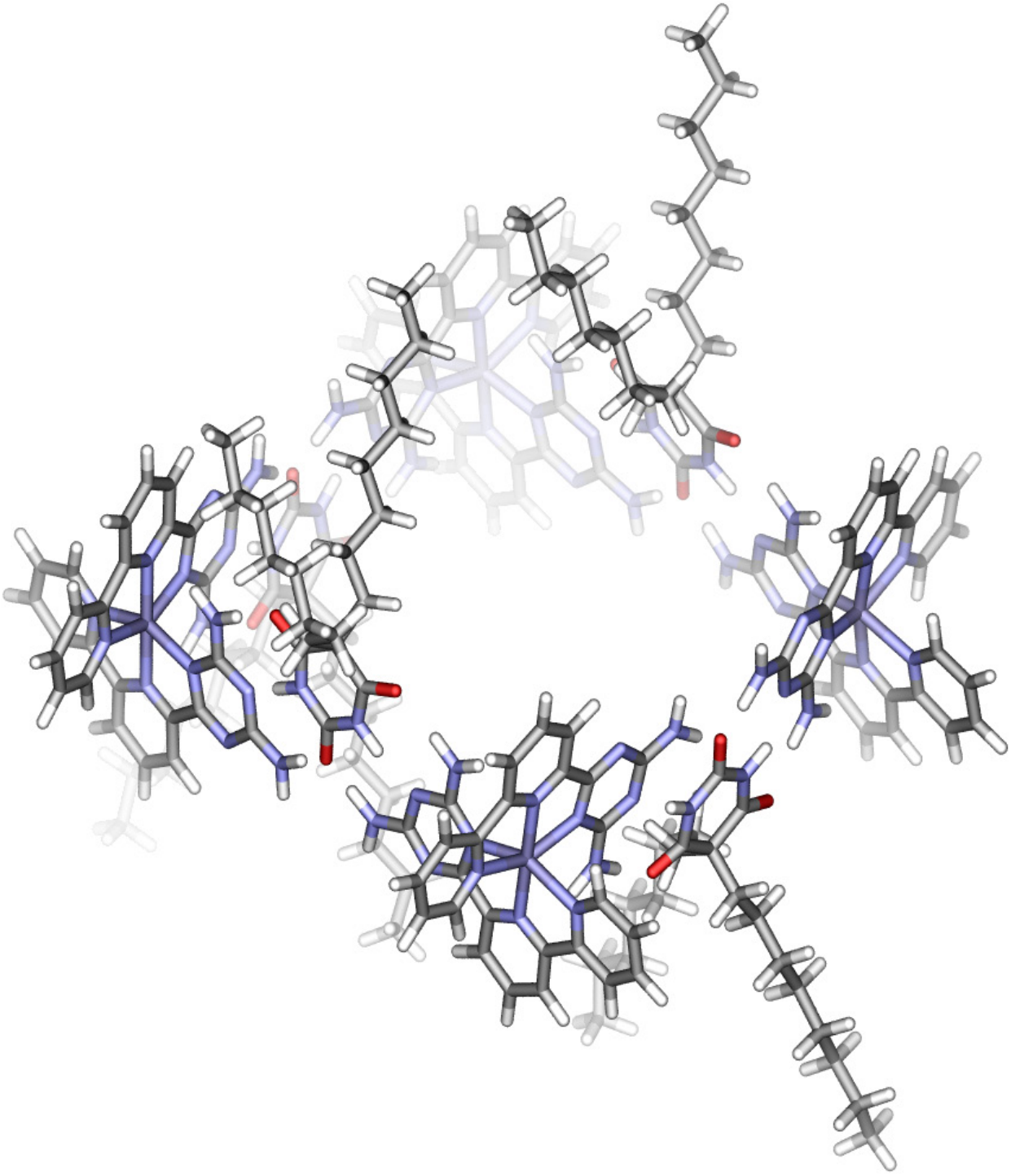

Figure S-31. Minimized structure of assembly $\{(\mathbf{1})_2 \bullet Fe\}^{2+}{}_4 \bullet \mathbf{2}_4$ from a tilted view, Fe-Fe distances ranging from 15.40 to 15.66 Å (SPARTAN, AM1 force field).

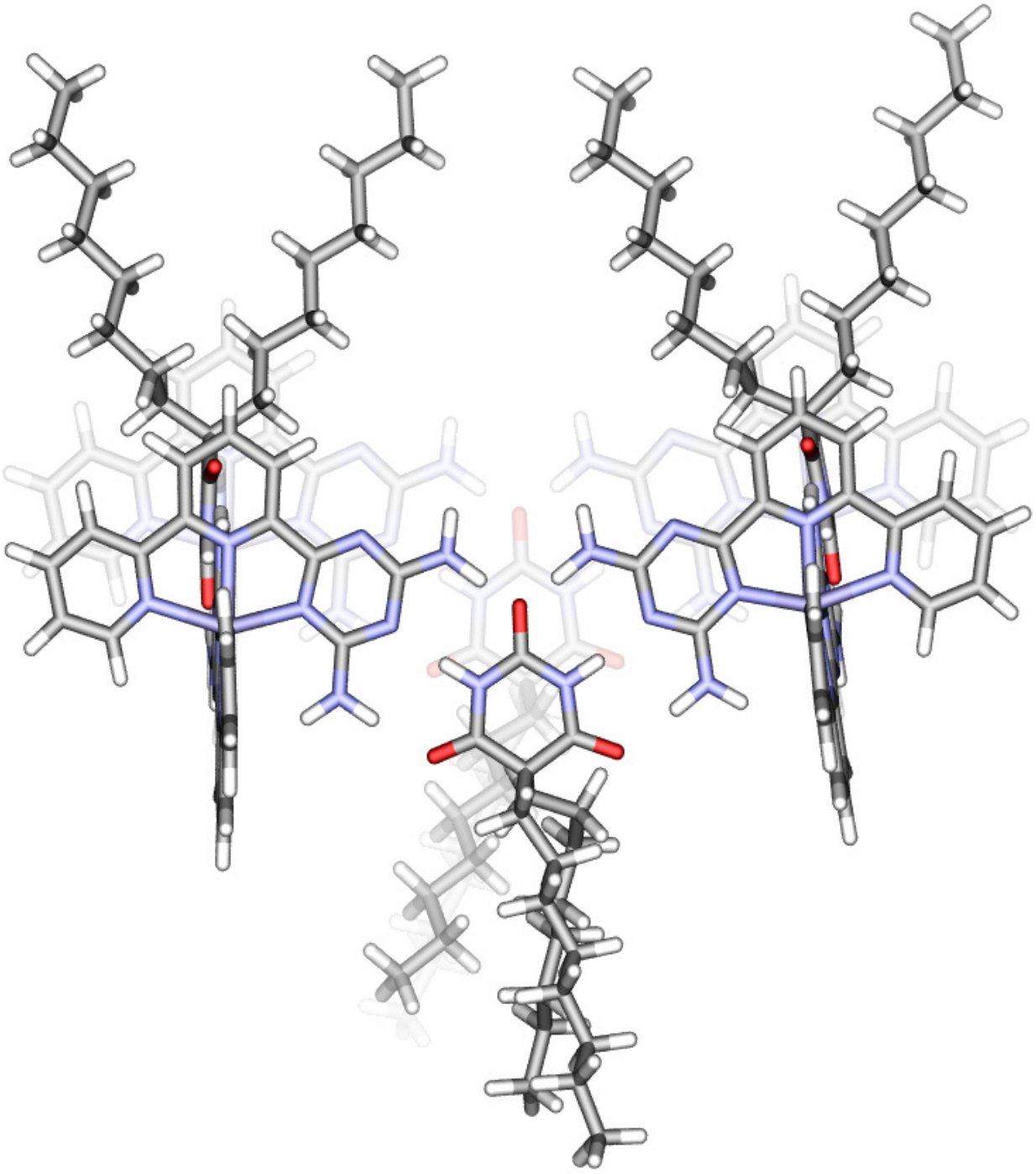

Figure S-32. Minimized structure of assembly $\{(\mathbf{1})_2 \bullet Fe\}^{2+}{}_4 \bullet \mathbf{2}_4$ from a side view, Fe-Fe distances ranging from 15.40 to 15.66 Å (SPARTAN**,** AM1 force field).

8. X-Ray Structure Determination

Complex $(1)_2$•Fe•$(ClO_4)_2$ CCDC Submission number 934197

A black prism fragment (0.46 x 0.33 x 0.06 mm^3) was used for the single crystal X-ray diffraction study of $[C_{13}H_{11}N_7]_2Fe]][ClO_4]_2 \cdot CH_3CN$. The crystal was coated with paratone oil and mounted on to a cryo-loop glass fiber. X-ray intensity data were collected at 100(2) K on a Bruker APEX2[3] platform-CCD x-ray diffractometer system (fine focus Mo-radiation, λ = 0.71073 Å, 50KV/35mA power). The CCD detector was placed at a distance of 5.0600 cm from the crystal.

A total of 3600 frames were collected for a sphere of reflections (with scan width of 0.3° in ω, starting ω and 2θ angles at –30°, and ϕ angles of 0°, 90°, 120°, 180°, 240°, and 270° for every 600 frames, 10 sec/frame exposure time). The frames were integrated using the Bruker SAINT software package[4] and using a narrow-frame integration algorithm. Based on a monoclinic crystal system, the integrated frames yielded a total of 66601 reflections at a maximum 2θ angle of 56.56° (0.75 Å resolution), of which 8277 were independent reflections (R_{int} = 0.0412, R_{sig} = 0.0234, redundancy = 8.0, completeness = 99.9%) and 6905 (83.4%) reflections were greater than 2σ(I). The unit cell parameters were, **a** = 21.4191(8) Å, **b** = 10.8147(4) Å, **c** = 15.1758(6) Å, **β** = 108.398(1)°, V = 3335.7(2) $Å^3$, Z = 4, calculated density D_c = 1.646 g/cm^3. Absorption corrections were applied (absorption coefficient μ = 0.688 mm^{-1}; max/min transmission = 0.9625/0.7426) to the raw intensity data using the SADABS program.[5]

The Bruker SHELXTL software package[6] was used for phase determination and structure refinement. The distribution of intensities (E^2-1 = 0.961) and systematic absent reflections indicated one possible space group, P2(1)/c. The space group P2(1)/c (#14) was later determined to be correct. Direct methods of phase determination followed by two Fourier cycles of refinement led to an electron density map from which most of the non-hydrogen atoms were identified in the asymmetric unit of the unit cell. With subsequent isotropic refinement, all of the non-hydrogen atoms were identified. There were one cation of $[C_{13}H_{11}N_7]_2Fe]^{2+}$, two anions of $[ClO_4]^-$, and one solvent molecule of CH_3CN present in the asymmetric unit of the unit cell. All the NH2-groups H-atoms were involved in intermolecular hydrogen bonding.

Atomic coordinates, isotropic and anisotropic displacement parameters of all the non-hydrogen atoms were refined by means of a full matrix least-squares procedure on F^2. The H-atoms were included in the refinement in calculated positions riding on the atoms to which they were attached, except for the NH_2-group H-atoms were refined unrestrained. The refinement converged at R1 = 0.0358, wR2 = 0.0867, with intensity I>2σ (I). The largest peak/hole in the final difference map was 0.566/-0.616 e/Å^3.

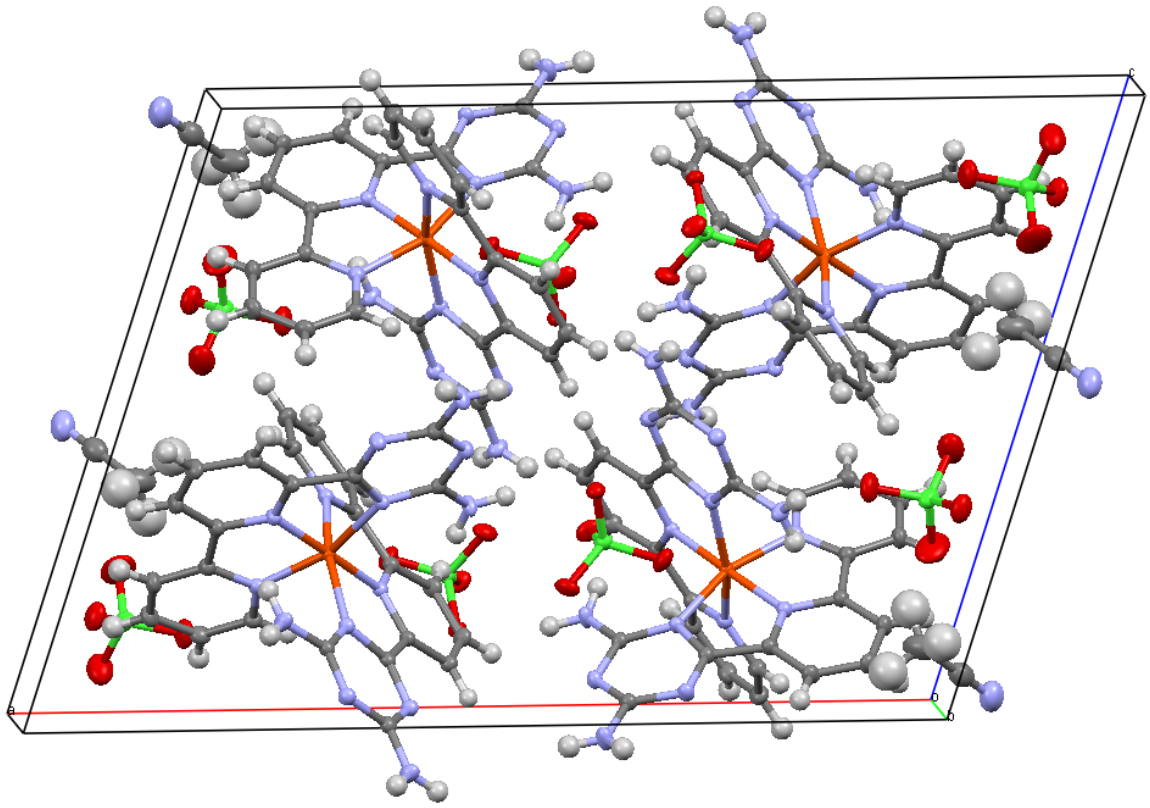

Figure S-33. Unit cell of (**1**)$_2$•Fe•(ClO$_4$)$_2$•CH$_3$CN crystal structure (100 °K).

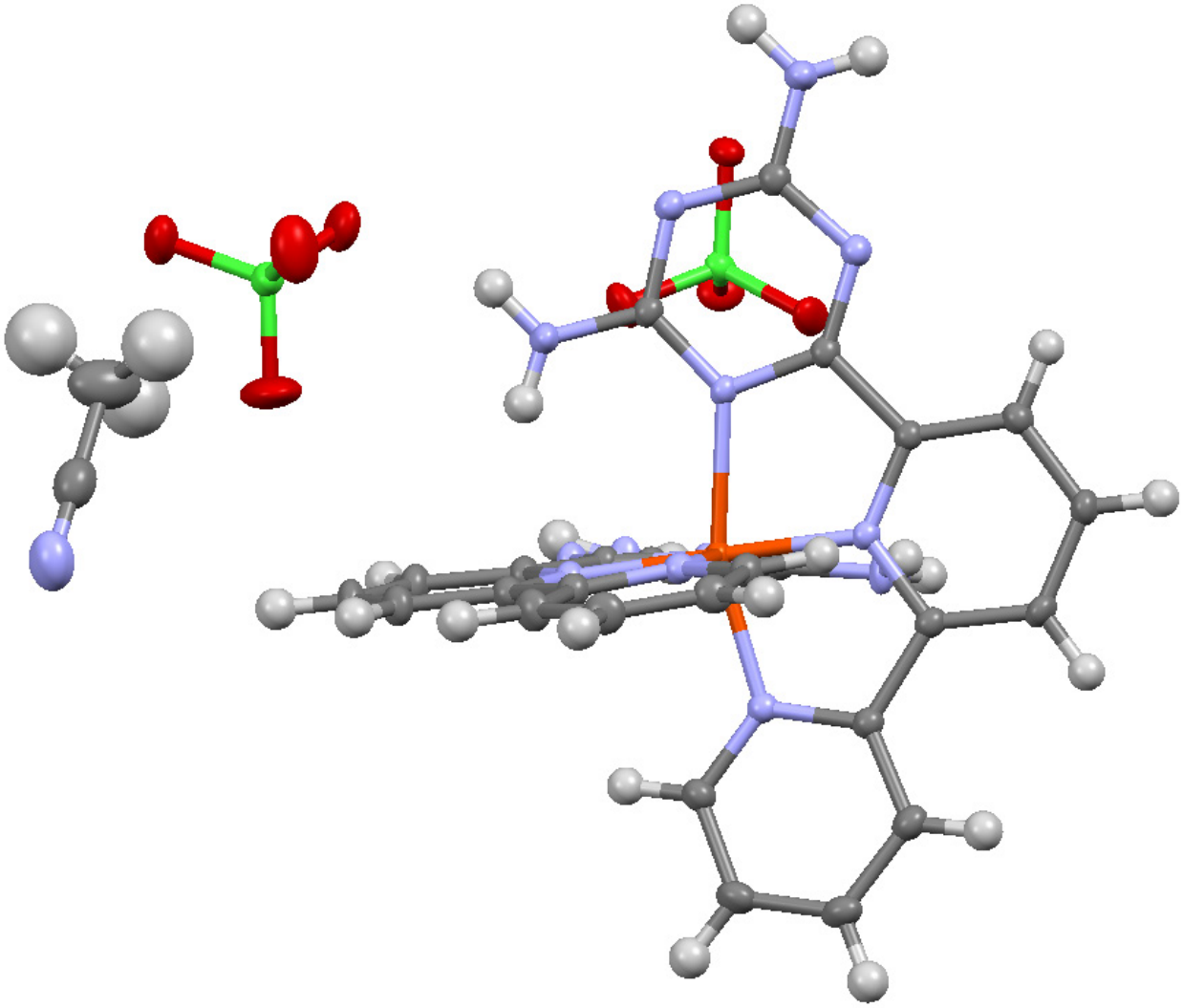

Figure S-34. Individual molecules of $(\mathbf{1})_2$•Fe•$(ClO_4)_2$•CH_3CN from the crystal structure (100 °K).

Table *S*-1. Crystal data and structure refinement for $(\mathbf{1})_2$•Fe•$(ClO_4)_2$•CH_3CN.

Empirical formula	$C_{28}\ H_{25}\ Cl_2\ Fe\ N_{15}\ O_8$	
Formula weight	826.38	
Temperature	100(2) K	
Wavelength	0.71073 Å	
Crystal system	Monoclinic	
Space group	P2(1)/c	
Unit cell dimensions	a = 21.4191(8) Å	α= 90°.
	b = 10.8147(4) Å	β= 108.3980(10)°.
	c = 15.1758(6) Å	γ = 90°.
Volume	3335.7(2) $Å^3$	
Z	4	
Density (calculated)	1.646 Mg/m^3	
Absorption coefficient	0.688 mm^{-1}	
F(000)	1688	
Crystal size	0.46 x 0.33 x 0.06 mm^3	
Theta range for data collection	2.00 to 28.28°.	
Index ranges	-28<=h<=28, -14<=k<=14, -20<=l<=20	
Reflections collected	66601	
Independent reflections	8277 [R(int) = 0.0412]	
Completeness to θ = 28.28°	99.9 %	
Absorption correction	Semi-empirical from equivalents	
Max. and min. transmission	0.9625 and 0.7426	
Refinement method	Full-matrix least-squares on F^2	
Data / restraints / parameters	8277 / 0 / 512	
Goodness-of-fit on F^2	1.031	
Final R indices [I>2σ (I)]	R1 = 0.0358, wR2 = 0.0867	
R indices (all data)	R1 = 0.0464, wR2 = 0.0926	
Largest diff. peak and hole	0.566 and -0.616 $e.Å^{-3}$	

References

1) (a) J. Loliger and R. Scheffold, *J. Chem. Educ.*, 1972, **49**, 646; (b) E. M. Schubert, *J. Chem. Educ.*, 1992, **69**, 62.
2) M. J. S. Dewar, E. G. Zoebisch, E. F. Healy, J. J. P. Stewart, *J. Am. Chem. Soc.*, 1985, **107**, 3902; calculations performed on SPARTAN 06, Wavefunction Inc.
3) *APEX 2,* version 2012.2.2, Bruker (2012), Bruker AXS Inc., Madison, Wisconsin, USA.
4) *SAINT,* version V8.18C, Bruker (2011), Bruker AXS Inc., Madison, Wisconsin, USA.
5) *SADABS,* version 2008/1, Bruker (2008), Bruker AXS Inc., Madison, Wisconsin, USA.
6) *SHELXTL,* version 2008/4, Bruker (2008), Bruker AXS Inc., Madison, Wisconsin, USA.